SEISMIC REFRACTION INTERPRETATION

BY

COMPUTER TECHNIQUE

AMNUAYCHAI THIENPRASERT

CONTENTS

ILLUSTRATIONS

Page

Page

TABLE

ATTACHED SHEETS

4. Model 4, printer plots showing time-distance graph and depth cross-section profiles with layer velocity specifications and without layer velocity specifications
5. Model 5, printer plots showing time-distance graph and depth cross-section profile
6. Model 6, printer plots showing time-distance graph and depth cross-section profile
7. Model 7, printer plots showing time-distance graph and depth cross-section profile which layer velocity specifications
8. Two layer seismic profile at New Mexico Tech.; the first problem profile, spreads A,B, and C
9. Two layer seismic profile at New Mexico Tech.; the second problem profile, spreads D,F, and G
10. Two layer seismic profile at New Mexico Tech.; the third problem profile, spreads H,J, and K

ACKNOWLEDGMENTS

The writer feels very much indebted to Dr. Allan R. Sanford for suggesting the problem, for his patient guidance and critical review of the manuscript. Thanks are also due to Dr. clifford R. Keizer and Dr. Marshall A. Reiter who served as my advisors and to Dr. Thomas A. Nartker and Dr. W. H. McMahan for helping some of the processing connected with this program which was run at the University of New Mexico Computer Center.

Special thanks are due to Mr. Steve Hughes, Mr. Robert Martinez and Mr. Steven Flint who made suggestions and corrected the computer program.

Finally, my appreciation is also extended to Mr. Carl Axness for correction of grammar and to Miss Theeranee Poonwiwat who helped on the key punching and typing.

ABSTRACT

The main body of my study concerns the modification of the Fortran Seismic Interpretation Program 1 (James H. Scott et al, 1972) from the Burroughs B-5500 computer to the IBM-360, including the testing of the program with various models. For a simple model, without too many structural irregularities the computer plots are fairly accurate. However, for more complex models it may be off by as much as 10 to 30 percent. In general the computer tends to smooth out sharp drops in the depth cross-section curve.

Included in my study is the computer interpretation of an 8,200 feet profile previously done by hand by Dr. Allan R. Sanford. His results only differed slightly in a few points from the computer interpretation. Other factors involved in the accuracy of the interpretation are the spread arrangements, the layer velocity control in each spread and the positions of the geophones, when the data is taken.

INTRODUCTION

Seismic refraction techniques have been used for decades to determine the depth of crustal layers and the structure of the earth crust but computations have usually been done by hand calculation. A computer program to interpret the seismic refraction data was published by the United States Department of The Interior, Bureau of Mines in 1972 under the title of "Computer Analysis of Seismic Refraction Data" by James H. Scott et al. The computer modeling technique can help the geophysicist to reduce the labor required to complete an interpretation.

This report is a study of the application of the computer program and its accuracy. By applying data problems that one gets from various structural models, and to study the technique for preparing sets of data decks and the spread arrangement, in order to get the highest precision posible.

THE SEISMIC REFRACTION THEORY

The main quantity measured in the seismic refraction method is the time between the initiation of the seismic wave and the first arrival of energy along the path between shot point and detectors. The first arrivals are evidences of the fastest traveling waves which are longitudinal waves. By observing first arrivals for a variety of shot detector distance, a time-distance curve can be constructed. The time-distance relations can be analyzed in terms of the variation with distance of minimum time paths. Then the elastic discontinuities can be deduced from these variations, and can be interpreted in terms of the nature, depth, and attitude of geologic units below the surface.

Ray Paths of Minimum Time

In a homogeneous, isotropic medium (Fig.1), a circular wave is initiated by an explosion at point a, which is on the surface. The longitudinal wave emitted travels with a velocity V_0. Let this medium overlie a second medium in which the wave travels with a higher velocity V_1.

Waves striking at the contact of these two velocity discontinuities will be partially reflected back into the upper medium and partially refracted into the lower medium. In general, the refractions take place according to Snell's law.

$$\sin i/\sin r = V_0/V_1 .$$

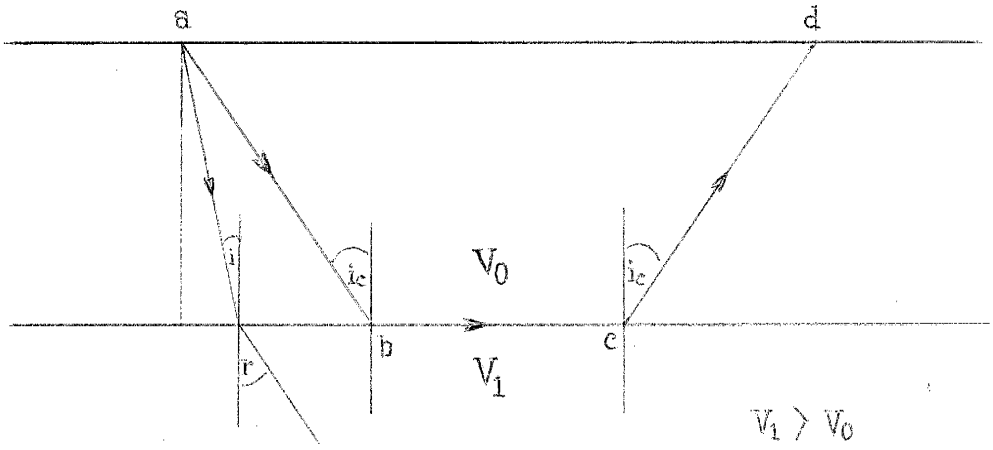

Fig.1 Refraction wave paths for a single horizontal velocity contrast.

Consider sin r=1, when the angle of refraction is 90 degrees. For this case, the incident angle is called "the critical angle"

$$\sin i_c = \frac{V_0}{V_1} .$$

The wave refracted at the critical angle i_c may be considered as a disturbance traveling along the surface of the second layer, with the velocity of the lower medium. The waves then travel upward and advance in the upper medium at the critical angle i_c. Thus, wave energy may be considered as going down to the surface of the discontinuity along a path ab, at the critical angle i_c, being refracted along that surface as bc and finally being refracted back to the surface of the ground along paths such as cd, again at the same critical angle i_c. The path abcd is a minimum time path.

Two Horizontal Layer Case

Consider the time-distance relations of the case of a single horizontal discontinuity at depth Z (Fig.2) between two media for which the wave travels at velocities of V_0 and V_1.

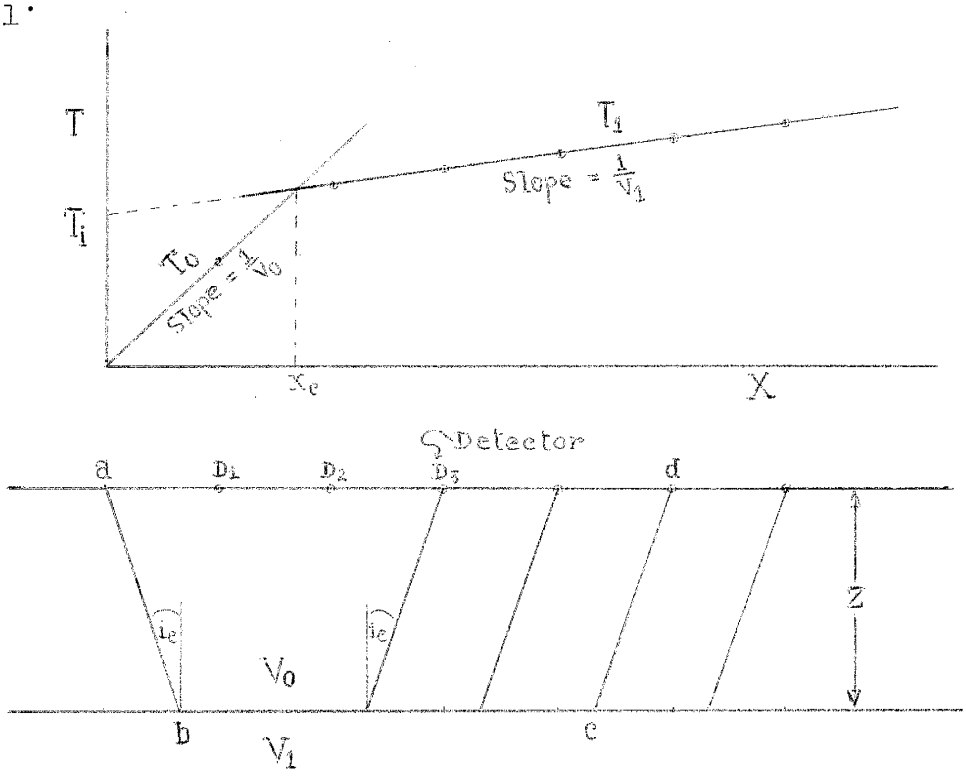

Fig.2 Minimum time path and time-distance curve for two layers.

The velocity of lower medium (V_1) is greater than the velocity of upper medium (V_0).

For the nearest detectors, the minimum time path is a ray directly from the source, travel horizontally in the upper medium, to the detector at the velocity V_0. So, the

time-distance curve starts out as a straight line through the origin with the slope $1/V_0$.

Let X be the horizontal distance from the source to the detector such that

$$T_0 = X/V_0.$$

At large distances from the source, the minimum time path is a ray that goes down to the surface of the discontinuity at the critical angle i_c at a velocity V_0, goes along the boundary at a velocity V_1, and then travels upward to the surface at the same critical angle i_c at a velocity V_0. The slope of the second part of the time-distance curve is $1/V_1$. The equation for the travel times of this phase can be obtained using the relations

$$\sin i_c = \frac{V_0}{V_1},$$

$$\cos i_c = \left(1 - \frac{V_0^2}{V_1^2}\right)^{\frac{1}{2}},$$

$$\cos i_c = \frac{(V_1^2 - V_0^2)^{\frac{1}{2}}}{V_1}, \quad \text{and}$$

$$\tan i_c = \frac{\sin i_c}{\cos i_c},$$

$$= \frac{V_0}{(V_1^2 - V_0^2)^{\frac{1}{2}}}.$$

Let T_1 be the total time along the refraction path abcd and X be the horizontal distance from the source to a detector. Then

$$
\begin{aligned}
T_1 &= T_{ab} + T_{bc} + T_{cd} , \\
&= \frac{ab}{V_0} + \frac{bc}{V_1} + \frac{cd}{V_0} , \\
&= \frac{Z}{V_0 \cos i_c} + \frac{X - 2Z \tan i_c}{V_1} + \frac{Z}{V_0 \cos i_c} , \\
&= \frac{2Z}{V_0 \cos i_c} - \frac{2Z \sin i_c}{V_1 \cos i_c} + \frac{X}{V_1} , \\
&= \frac{2Z}{V_0 \cos i_c} \left(1 - \frac{V_0 \sin i_c}{V_1} \right) + \frac{X}{V_1} , \\
&= \frac{2Z}{V_0 \cos i_c} \left(1 - \sin^2 i_c \right) + \frac{X}{V_1} , \\
&= \frac{X}{V_1} + \frac{2Z \left(V_1^2 - V_0^2 \right)^{\frac{1}{2}}}{V_1 V_0} . \qquad (1)
\end{aligned}
$$

We can now calculate the depth Z in various ways. The normal procedure is to use either the critical distance x_c or the intercept time T_i.

Depth From The Critical Distance

The critical distance x_c is the horizontal distance from the source that a wave which follows the refracted path will reach the surface at the same time as the one that traveled

the direct path.

At the critical distance x_c, $T_0 = T_1$, and thus

$$\frac{x_c}{V_0} = \frac{x_c}{V_1} + \frac{2Z(V_1^2 - V_0^2)^{1/2}}{V_1 V_0}, \qquad \text{from which}$$

$$Z = \frac{x_c}{2}\left(\frac{1}{V_0} - \frac{1}{V_1}\right)\frac{V_1 V_0}{\sqrt{V_1^2 - V_0^2}},$$

$$= \frac{x_c}{2}\frac{V_1 - V_0}{\sqrt{V_1^2 - V_0^2}},$$

$$= \frac{x_c}{2}\sqrt{\frac{V_1 - V_0}{V_1 + V_0}}. \qquad (2)$$

Depth From The Intercept Time

At the zero distance (X=0), the slope of $1/V_1$ of time-distance curve will intercept the time axis at T_i. From equation (1),

$$T_i = \frac{2Z\sqrt{V_1^2 - V_0^2}}{V_1 V_0}, \qquad \text{and}$$

$$Z = \frac{T_i}{2}\frac{V_1 V_0}{\sqrt{V_1^2 - V_0^2}}, \qquad (3)$$

or $$Z = \frac{TV_0}{2} \Big/ \left(1 - \frac{V_0^2}{V_1^2}\right)^{1/2}. \qquad (4)$$

The Delay Time

The delay time for any segment of the ray trajectory is defined as the additional time for the wave to travel that segment over the time which would be required to travel the horizontal component of that segment at highest velocity reached by the trajectory.

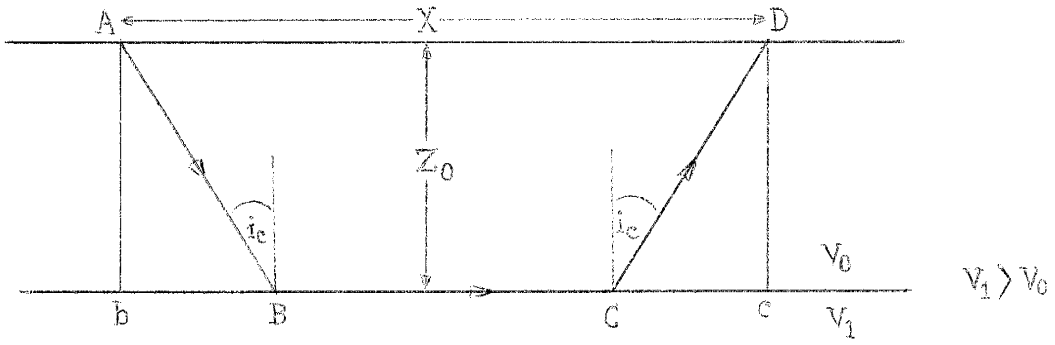

Fig.3 Delay time.

In the figure 3, the delay time is the travel time along the segment AB of the wave path at velocity V_0 minus the time require to travel the distance bB at velocity V_1. Thus, the delay time D_1 is

$$D_1 = \frac{AB}{V_0} - \frac{bB}{V_1} ,$$

$$= \frac{Z_0}{V_0 \cos i_c} - \frac{Z_0 \tan i_c}{V_1} ,$$

$$D_1 = \frac{Z_0}{V_0 \cos i_c} - \frac{Z_0 \sin i_c}{V_1 \cos i_c} ,$$

$$= \frac{Z_0}{V_0 \cos i_c} - \frac{Z_0 \sin^2 i_c}{V_0 \cos i_c} ,$$

$$= \frac{Z_0}{V_0 \cos i_c} (1 - \sin^2 i_c) ,$$

$$= \frac{Z_0 \cos i_c}{V_0} ,$$

$$= \frac{Z_0 \sqrt{V_1^2 - V_0^2}}{V_0 V_1} . \qquad (5)$$

The time for a refracted wave path ABCD is the time required to travel the distance X at velocity V_1 plus the delay times for the two slant segments, i.e.

$$T_1 = \frac{X}{V_1} + 2D_1 ,$$

$$= \frac{X}{V_1} + \frac{2Z_0 \cos i_c}{V_0} . \qquad (6)$$

Multiple Horizontal Layer Case

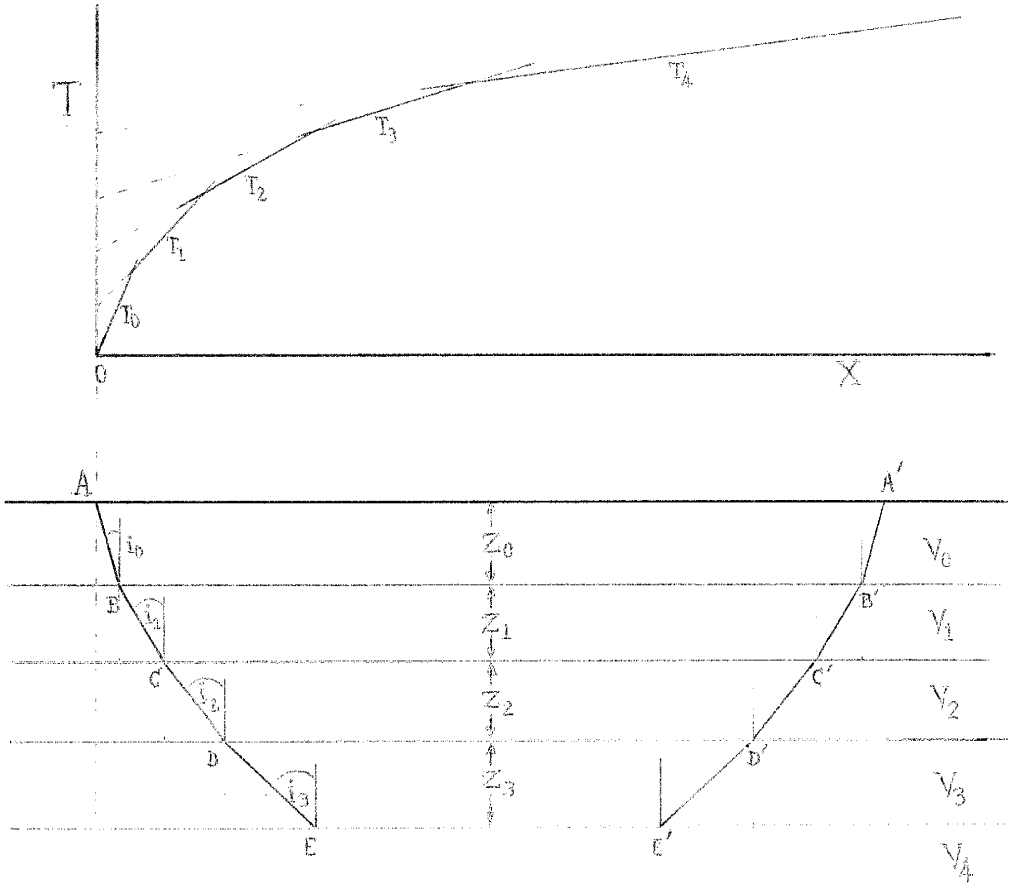

Fig.4 Multiple horizontal layer case.

Consider the multiple layer case in the figure 4 which the strata consists of several horizontal layers of thicknesses Z_0, Z_1, Z_2, etc., of successively increasing velocities V_0, V_1, V_2, etc.. The paths of rays penetrating to various beds and refracted at the discontinuities are determined by Snell's law. The delay time for each layer can be determined and the travel time along the path ABCDEEDCBA

can be computed by substituting the delay time of each layer. By Snell's law

$$\sin i_3 = V_3/V_4$$

$$\sin i_2 = (V_2/V_3)\sin i_3 = V_2/V_4$$

$$\sin i_1 = (V_1/V_2)\sin i_2 = V_1/V_4$$

$$\sin i_0 = (V_0/V_1)\sin i_1 = V_0/V_4$$

There fore;

$$\cos i_3 = \sqrt{1 - (V_3/V_4)^2}$$

$$\cos i_2 = \sqrt{1 - (V_2/V_4)^2}$$

$$\cos i_1 = \sqrt{1 - (V_1/V_4)^2}$$

$$\cos i_0 = \sqrt{1 - (V_0/V_4)^2}$$

The travel times for the various wave paths, in terms of delay times are;

$$T_0 = \frac{X}{V_0}$$

$$T_1 = \frac{X}{V_1} + 2D_1$$

$$T_2 = \frac{X}{V_2} + 2D_2 + 2D_1$$

$$T_3 = \frac{X}{V_3} + 2D_3 + 2D_2 + 2D_1$$

The total time of the wave along the paths ABCDEEDCBA in terms of delay times can be expressed as

$$T_4 = \frac{X}{V_4} + 2D_1 + 2D_2 + 2D_3 + 2D_4$$

$$= \frac{X}{V_4} + \frac{2Z_0 \cos i_1}{V_0} + \frac{2Z_1 \cos i_2}{V_1} + \frac{2Z_2 \cos i_3}{V_2} + \frac{2Z_3 \cos i_4}{V_3}$$

$$= \frac{X}{V_4} + \frac{2Z_0\sqrt{V_4^2 - V_0^2}}{V_0 V_4} + \frac{2Z_1\sqrt{V_4^2 - V_1^2}}{V_1 V_4} + \frac{2Z_2\sqrt{V_4^2 - V_2^2}}{V_2 V_4} + \frac{2Z_3\sqrt{V_4^2 - V_3^2}}{V_3 V_4} \quad (8)$$

Thus, the general expression for the time of a ray penetrating to a layer n can be written.

$$T_n = \frac{X}{V_n} + 2\sum_{m=0}^{n} \frac{Z_m\sqrt{V_n^2 - V_m^2}}{V_m V_n} \quad (9)$$

Non-horizontal Surfaces

In the situation of structural irregularities, such as, in the case of the shot point and the seismic detector different elevations or inclined velocity discontinuities, the travel times can be computed in several ways.

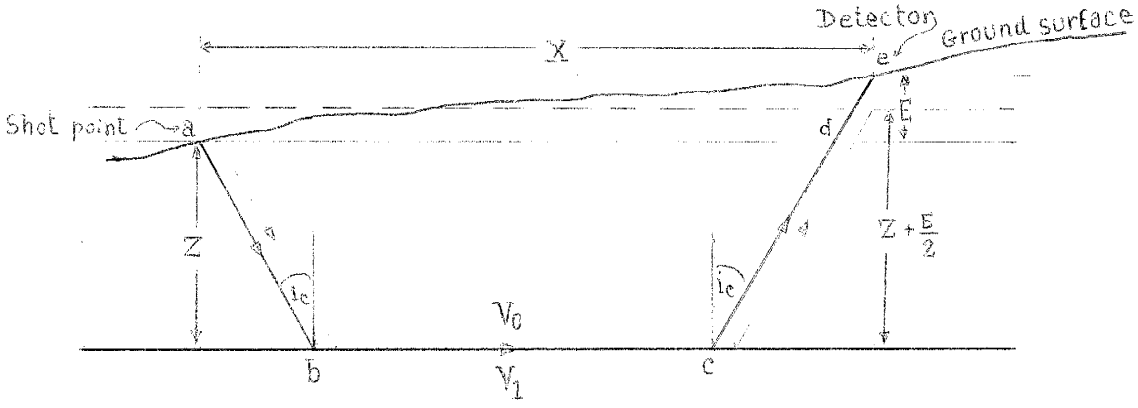

Fig.5 Shot point and detector at different elevations.

Shot Point and Detector at Different Elevations. Consider the case in which the receiver is at a height E (Fig.5) above the shot point. The travel times along the path abcde is the same as the travel times along the path abcd and the path de.

The delay time along the path de = $(E\cos i_c)/V_0$, and therefore, the total travel time will be

$$T_1 = \frac{X}{V_1} + \frac{2Z\cos i_c}{V_0} + \frac{E\cos i_c}{V_0} ,$$

$$= \frac{X}{V_1} + \frac{(2Z+E)\cos i_c}{V_0} . \qquad (10)$$

The time is the same as if shot point and detector were at the average elevation of the two. The depth from this mean elevation to the velocity discontinuity will be $Z+\frac{E}{2}$.

Dipping Interfaces. In this case, the velocity discontinuity is dipping at an angle Θ with respect to the horizontal. The shot points S_1 and S_2 on opposite end of a spread (Fig.6a and Fig.6b) will generate elastic waves which travel along downdip and updip paths. The apparent velocity of a wave refracted along the updip path is greater than the apparent velocity of a wave refracted along the downdip path.

Consider first the case in which the slope is downward from the shot point toward the detector (Fig.6a). This situation is like the case of shot point and detector at different elevations except that the surface of the ground is horizontal at distance X and the distance parallel to the

sloping surface is Xcos θ.

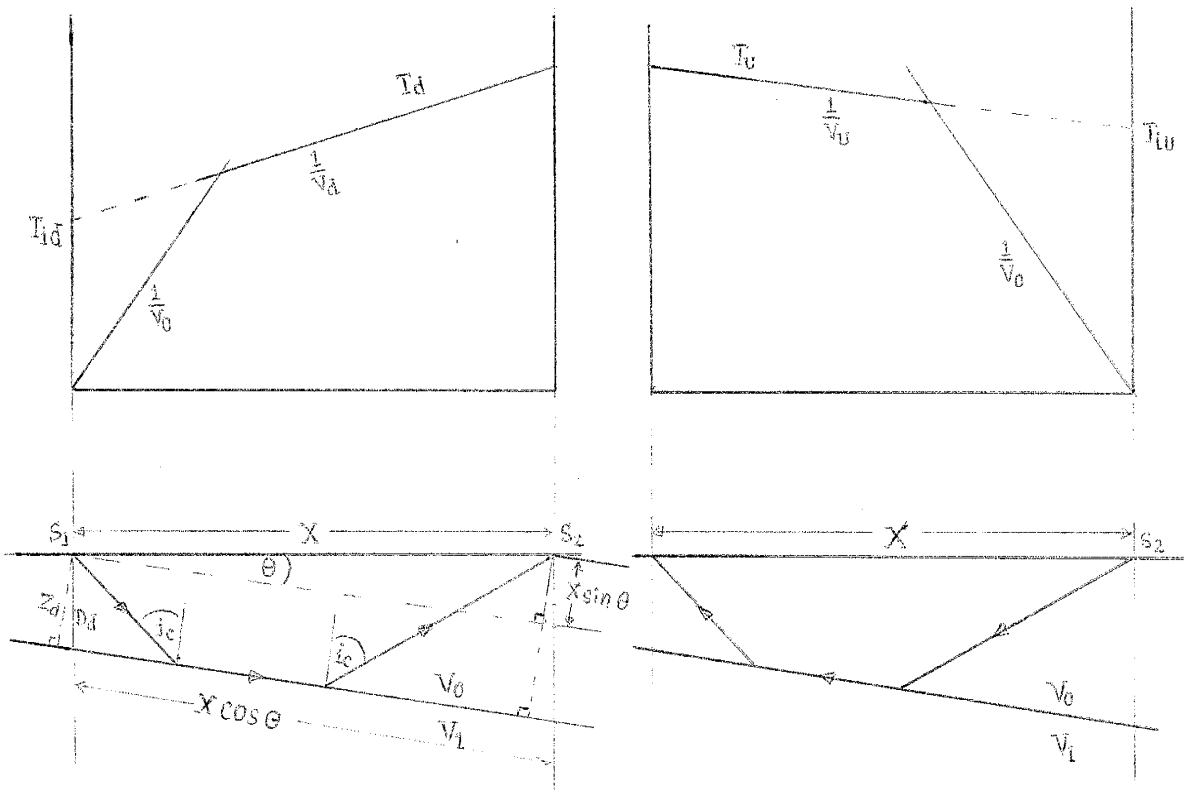

Fig.6a and Fig.6b Dipping interfaces.

The depth Z_d is measured perpendicular to the sloping bed from the shot point at the updip end. The distance corresponding to the difference in elevation becomes Xsin θ. Therefore, eq. (10) becomes

$$T_d = \frac{X \cos \theta}{V_1} + \frac{(2Z_d + X \sin \theta) \cos i_c}{V_0} \quad ,$$

Substituting $V_1 = V_0/\sin i_c$ gives

$$T_d = \frac{2Z_d \cos i_c}{V_0} + \frac{X \cos \theta \sin i_c}{V_0} + \frac{X \sin \theta \cos i_c}{V_0} \quad ,$$

$$T_d = \frac{2Z_d \cos i_c}{V_0} + \frac{X}{V_0}(\cos\theta \sin i_c + \sin\theta \cos i_c),$$

$$= \frac{2Z_d \cos i_c}{V_0} + \frac{X}{V_0} \sin(i_c + \theta). \qquad (11)$$

The slope of the T_d segment of the time-distance curve is

$$\frac{1}{V_d} = \frac{\sin(i_c + \theta)}{V_0} = \frac{\sin(i_c + \theta)}{V_1 \sin i_c}. \qquad (12)$$

Similarly, the updip time is

$$T_u = \frac{2Z_u \cos i_c}{V_0} + \frac{X}{V_0} \sin(i_c - \theta), \qquad (13)$$

Where Z_u is the perpendicular distance to the interface from the shot point at the downdip end of the line.

The slope of T_u segment is

$$\frac{1}{V_u} = \frac{\sin(i_c - \theta)}{V_0} = \frac{\sin(i_c - \theta)}{V_1 \sin i_c} \qquad (14)$$

From equations (12) and (13), it is obvious that V_u is greater than V_d. Both V_u and V_d are apparent velocities of the second layer. The true velocity (V_1) and the dip angle (θ) of this layer can be determined from the addition of equations (12) and (14)

$$\frac{V_0}{V_d} + \frac{V_0}{V_u} = \sin(i_c+\theta) + \sin(i_c-\theta),$$

$$= 2\sin i_c \cos\theta.$$

Substituting $\sin i_c = V_0/V_1$ gives

$$\frac{V_0}{V_d} + \frac{V_0}{V_u} = \frac{2V_0 \cos\theta}{V_1}$$

$$V_1 = \frac{2\cos\theta}{\frac{1}{V_d} + \frac{1}{V_u}} \tag{15}$$

Now $i_c + \theta = \sin^{-1}\frac{V_0}{V_d}$, and

$$i_c - \theta = \sin^{-1}\frac{V_0}{V_u},$$

Therefore $$\theta = \frac{1}{2}\left[\sin^{-1}\frac{V_0}{V_d} - \sin^{-1}\frac{V_0}{V_u}\right] \tag{16}$$

Depth to the interface can be calculated by using the intercept time in a similar way to the procedure used for horizontal beds, i.e.,

$$T_{id} = \frac{2Z_d \cos i_c}{V_0}, \tag{17}$$

$$Z_d = \frac{V_0 T_{id}}{2\cos i_c} \tag{18}$$

A similar expression is obtained for Z_u in the term of T_{iu}.

The depth to the interface directly below the shot point will be $D_d = Z_d/\cos\theta$ while $D_u = Z_u/\cos\theta$, where θ is the dip.

Faulted Beds. Consider the case when a high-velocity bed is faulted down. The first arrivals of the refracted wave along a line across the fault will have a second break in the time-distance curve.

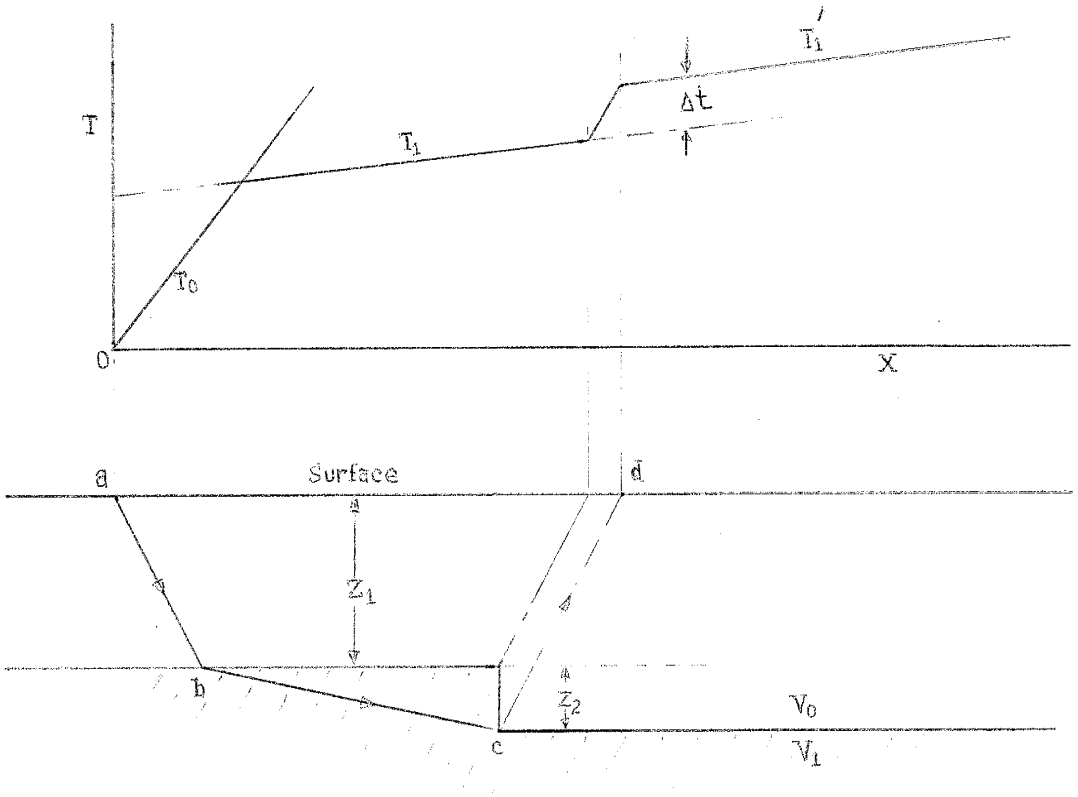

Fig.7 Fault with finite displacement and corresponding time-distance curve for shot point on upthrow side of fault.

For the case where the shot point is on the upthrown side (Fig.7), and Z_2 is small compare with the horizontal distances of the diagram, we may consider that the time for the path bc is approximately the same as if this were the horizontal distance, then

$$T_1' = \frac{X}{V_1} + \frac{Z_1 \cos i_c}{V_0} + \frac{(Z_1 + Z_2) \cos i_c}{V_0}, \text{ and} \qquad (19)$$

$$T_1 = \frac{X}{V_1} + \frac{2 Z_1 \cos i_c}{V_0} . \qquad (20)$$

The offset in the time-distance curve by the displace-

ment Z_2 can be expressed as

$$\Delta t = T_1' - T_1 ,$$

$$= \frac{Z_2 \cos i_c}{V_0} .$$

The throw Z_2 is

$$Z_2 = \frac{\Delta t V_0}{\cos i_c} = \frac{\Delta t V_0 V_1}{\sqrt{V_1^2 - V_0^2}} . \qquad (21)$$

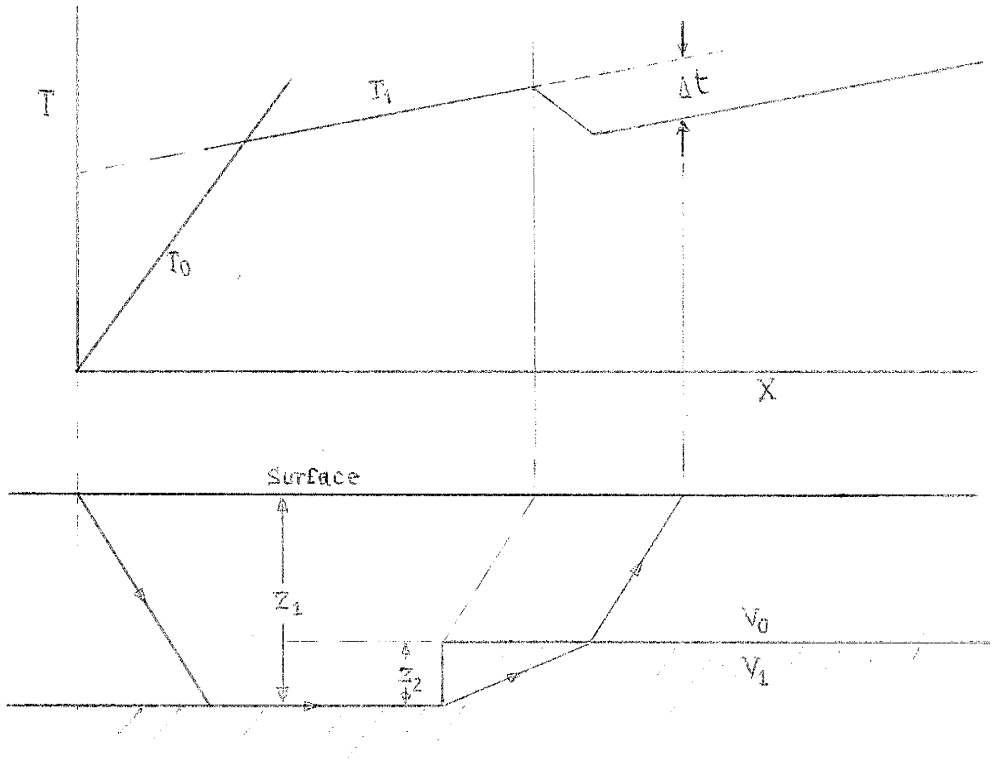

Fig.8 Fault with finite displacement and corresponding time-distance curve for shot point on downthrow side of fault.

Consider now the case where the shot point is on the drownthrown side and the detector is on the upthrown side

(Fig.8). The time-distance curve is derived in a similar way but the offset in the linear segment will be a drownward break.

DESCRIPTION OF THE COMPUTER PROGRAM AND METHOD OF CALCULATION

The computer program FSIP1 (Fortran Seismic Interpretation Program 1) for seismic refraction modeling is designed for a Burroughs B-5500 computer. This computer program is very useful because for many refraction surveys the labor requirement is too lengthy and too monotonous for calculation to be performed by hand.

The first step in this study was to modify this computer program to be capable with the IBM-360 computer which is in use at the University of New Mexico. Then, data for six models were applied to the program.

The program is limited to interpretation of data from 1 to 5 in line spreads with up to 7 shot points and 12 geophones each, and for as many as 5 layers with layer velocity increasing with layer depth. The general structure of the program is described in three parts as shown on the block diagram.

PART 1 : The computer reads and stores the input information for the problem. Then all input information is printed out again in tabular form, so that it can be easily checked and verified again. The first exit point in the program (EXIT 0) provides the interpreter with a sample time-distance graph of the observed travel times plotted against horizontal distances between shot points and detectors.

Next, the program estimates the velocity of the surface layer by averaging the individual velocity values indicated by direct-arrival from shot points to geophones. Then this velocity is used for computing time corrections that reference all refracted rays to the datum plane. Another time-distance graph of the datum-corrected travel times can be plotted on the EXIT 1 option. Plotting of this graph completes part 1 of the program.

PART 2 : The velocity of layer 2 is estimated by two methods. The first method is equivalent to drawing a line through points of a time-distance graph and determining the inverse slope of the line. The second method used to estimate velocity was developed by the Geological Survey of Canada (Hobson and Overton, 1968). The estimate is made by use of the following formular:

$$v = \frac{\Sigma \Delta x_i^2 - (\Sigma \Delta x_i)^2/n}{\Sigma \Delta x_i \Delta t_i - (\Sigma \Delta x_i)(\Sigma \Delta t_i)/n}$$

when v is the desired refraction velocity,

Δx_i is the difference between distance to geophone i from shot points on opposite ends the spread,

Δt_i is the difference between arrival times at geophone i from the same two opposing shot points,

and n is the total number of geophones used in the computation.

After the velocity of layer 2 is established, the pro-

gram estimates the position of the base of the surface layer by a computer adaptation of the delay time method. Then the accuracy of this result is improved by the ray-tracing technique.

The delay time depth points are computed for each geophone which receives the refracted waves along the interface between layer 1 and 2. If more than one depth point is available at a geophone, the depth values are averaged to establish a better estimate of the position directly beneath each geophone. For geophones with missing values, depth points are established by interpolation or extrapolation from available points nearby. Then this initial depth estimate is tested for validity by a one pass ray-tracing procedure and subsequent adjustment. Starting from each depth point previously established, rays are traced upward from the velocity discontinuity to the actual positions of shot points and geophones. The direction of each ray is established by Snell's law from the velocities of layers 1 and 2, and from the dip of the segmented line representing the discontinuity at the specified points.

Interpolation or extrapolation is established for the position adjustment of rays missing the target geophones or shot points. The total travel time of the ray from shot point to geophone can be computed by adding the time for the ray traveling along the discontinuity to travel times for the slant segment. This computed time is then compared with

the travel time, and the estimated points of entry and emergence of each ray are adjusted upward to absorb the discrepancy. When this adjustment has been made for all geophones, new depths are established by averaging to define the plane beneath each geophone.

Next, the travel times associated with the slant ray-segments in the surface layer are substracted from all observed arrival times, and the velocities of all layers beneath layer 2 are estimated by the regression technique and the Hobson-Overton technique described previously. When this is completed, the user can obtain a plot of the time-distance graph with layer 1 removed by selecting the EXIT 2 option of the program.

PART 3 : If the EXIT 2 is not selected, the program proceeds to delineate layers beneath layer 2. With layer 1 removed, the delay time technique is used again to obtain a first approximation of the bases beneath layer 2. Coordinates of points of the slant-ray-segments are computed and are averaged. The computer connects these average points together with straight line segments and finds the intersections that occur with vertical lines projected downward from each geophone position. These intersections are used as the first approximation that defines the top of the layer being delineated. Any missing point beneath a geophone resulting from insufficient data are filled again by interpolation or extrapolation from nearby locations where informtion is available.

At this point the user can obtain the first plot of the depth cross-section by selecting the EXIT 3 option.

The accuracy of the delay time first approximation is tested by ray tracing in a manner similar to that described previously, except that rays are traced through all layers between the discontinuity and the geophones or short points. Computed times associated with traced rays are compared with observed travel times, and the positions of ray end points are adjusted to absorb the discrepancies. Then the layer is resmoothed and some of missing points are filled in again. This completes the first iteration of ray-tracing and adjustment. Another depth cross-section plot can be obtained by selecting the EXIT 4 option of the program.

The first iteration of ray-tracing and adjustment is followed by a second one. On the second pass, the direction of the initial ray segments are determined for each individual ray by using the actual dip at the point of the interest on the smoothed model interface. For two iterations of ray-tracing and adjustment the EXIT 5 option may be selected to plot one more cross-section depth.

Now, the final adjustment is made from the base of layer 1 to remove the effects of small errors in the position of this shallow layer. These small errors are transferred to deeper interfaces with magnification because of increased velocity with depth. After the base of layer 1 is repositioned beneath each geophone and shot point, the program goes

through one final pass of ray- tracing and adjustment for all deeper layers. This completes the computation part of the program, and selecting EXIT 6 obtains the result of the full computation which includes the delay-time approximation, two iterations of ray-tracing, and adjustment followed by correlated error correction of the layer 1 and finally by one last iteration of ray-tracing and adjustment for each layer.

BLOCK DIAGRAM

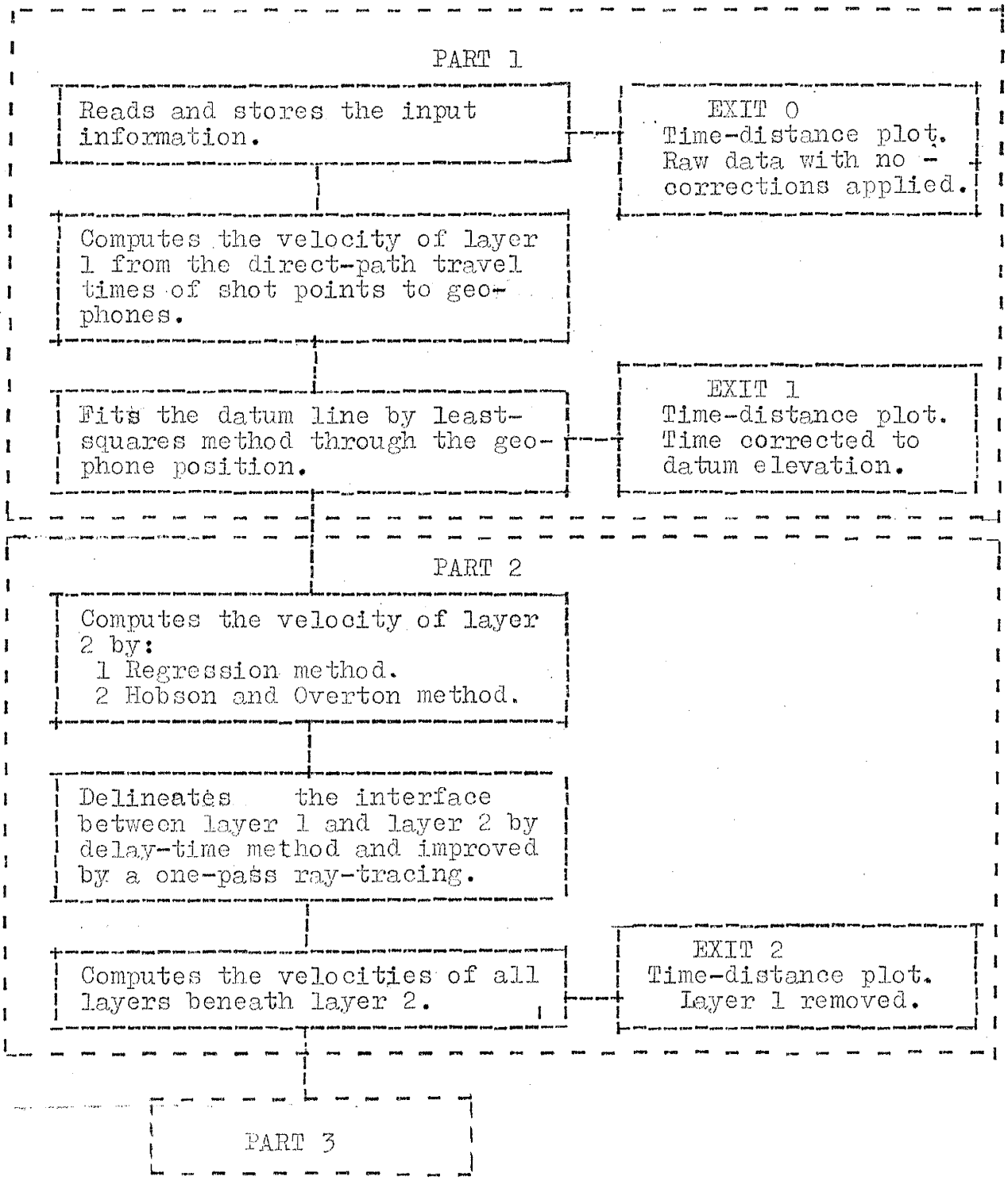

Table 1. Block diagram shows the procedure of the computation.

BLOCK DIAGRAM (continued)

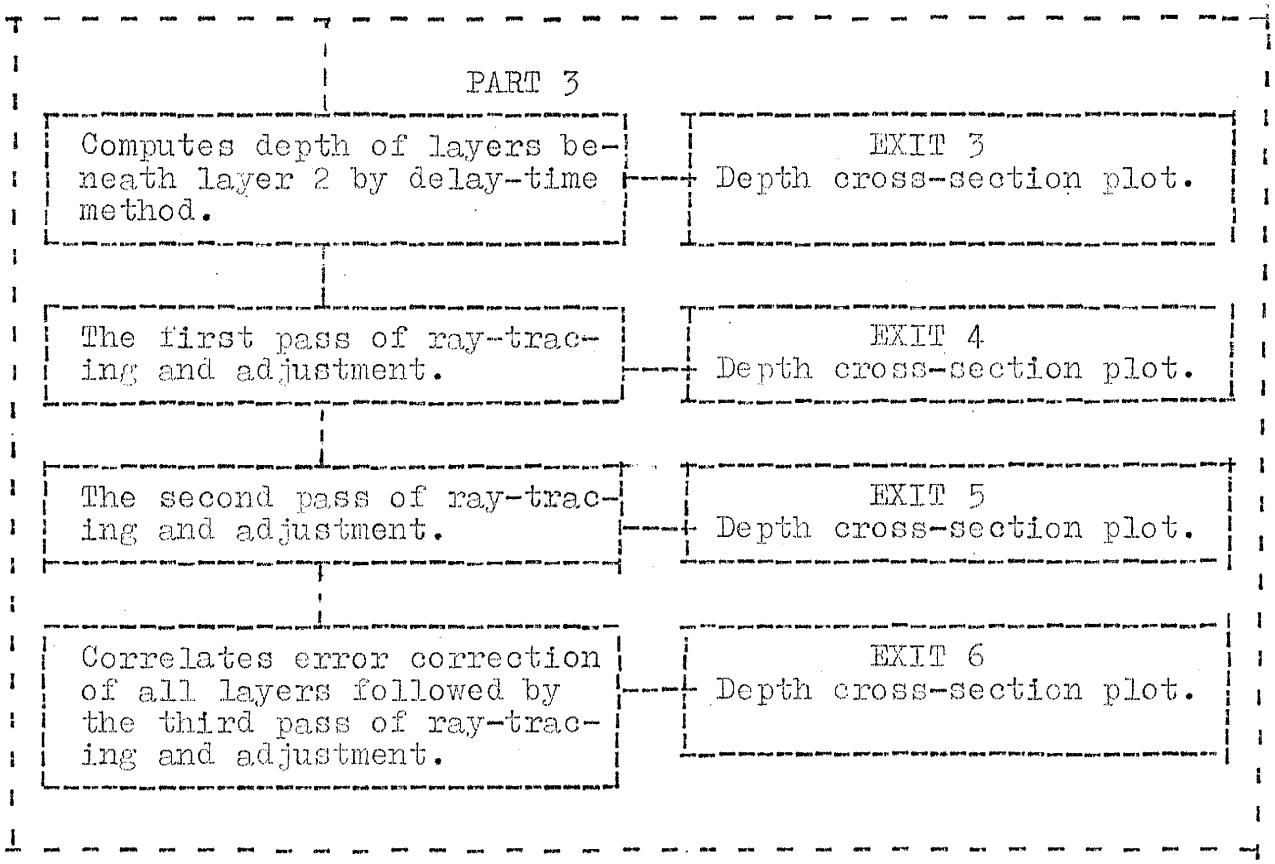

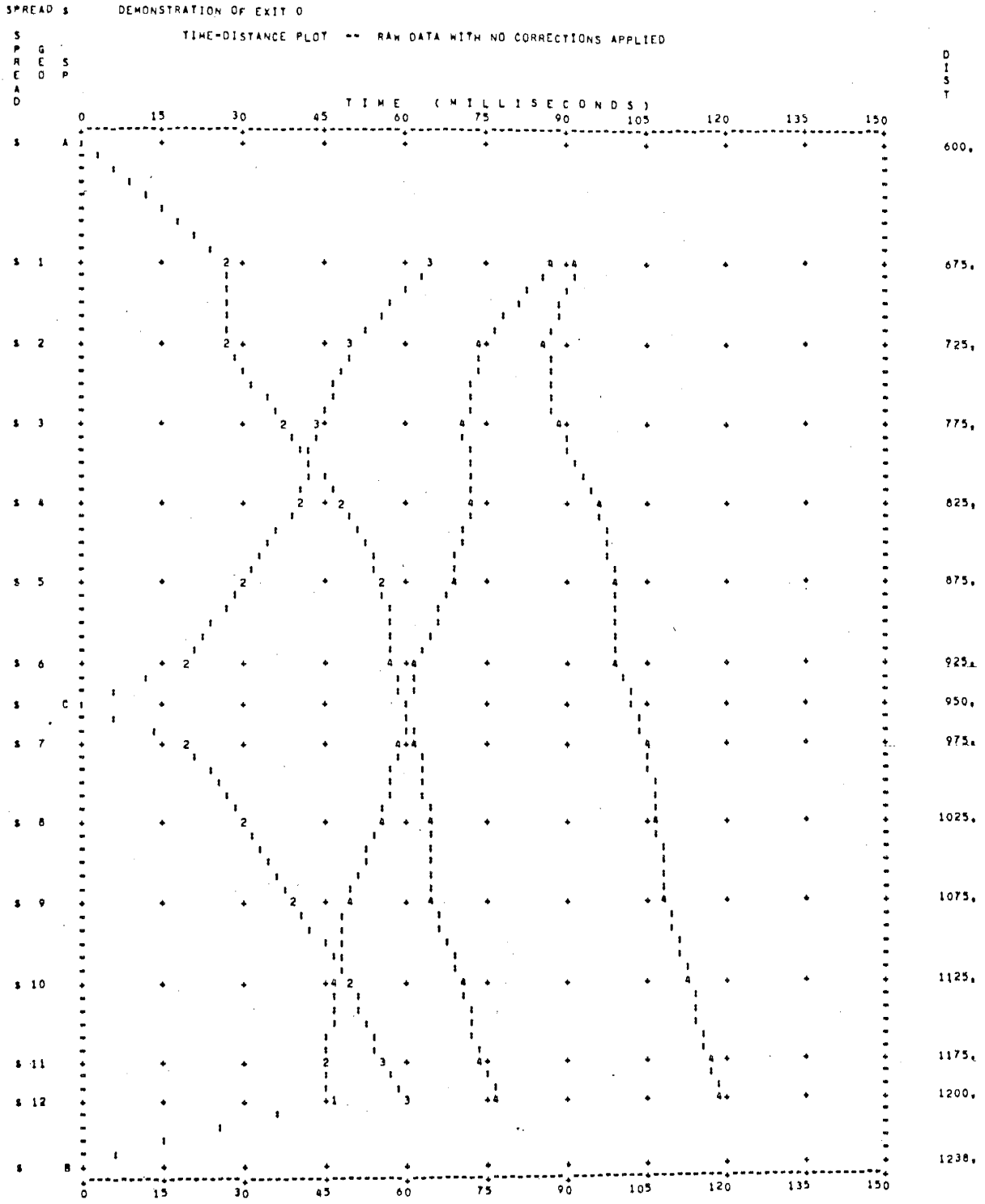

FIGURE 9.- Printer Plot, Program FSIP1 EXIT = 0, Showing Observed Travel Times Plotted Against Shot Point-Geophone Distances, No Corrections Applied.

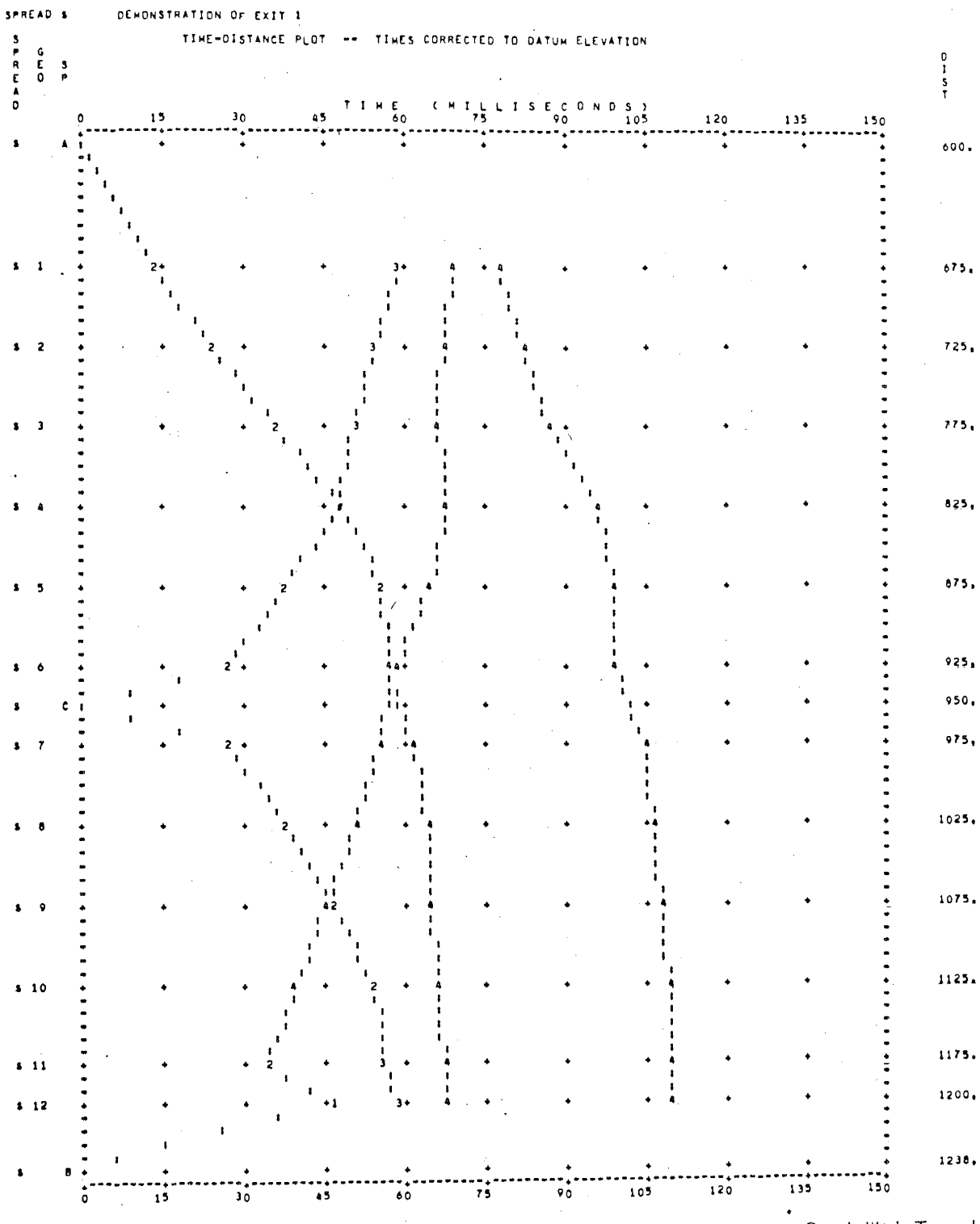

FIGURE 10. Printer Plot, Program FSIP1 EXIT 1, Showing Time-Distance Graph With Travel Times Corrected for Terrain Irregularity and Referenced to a Sloping Datum Plane.

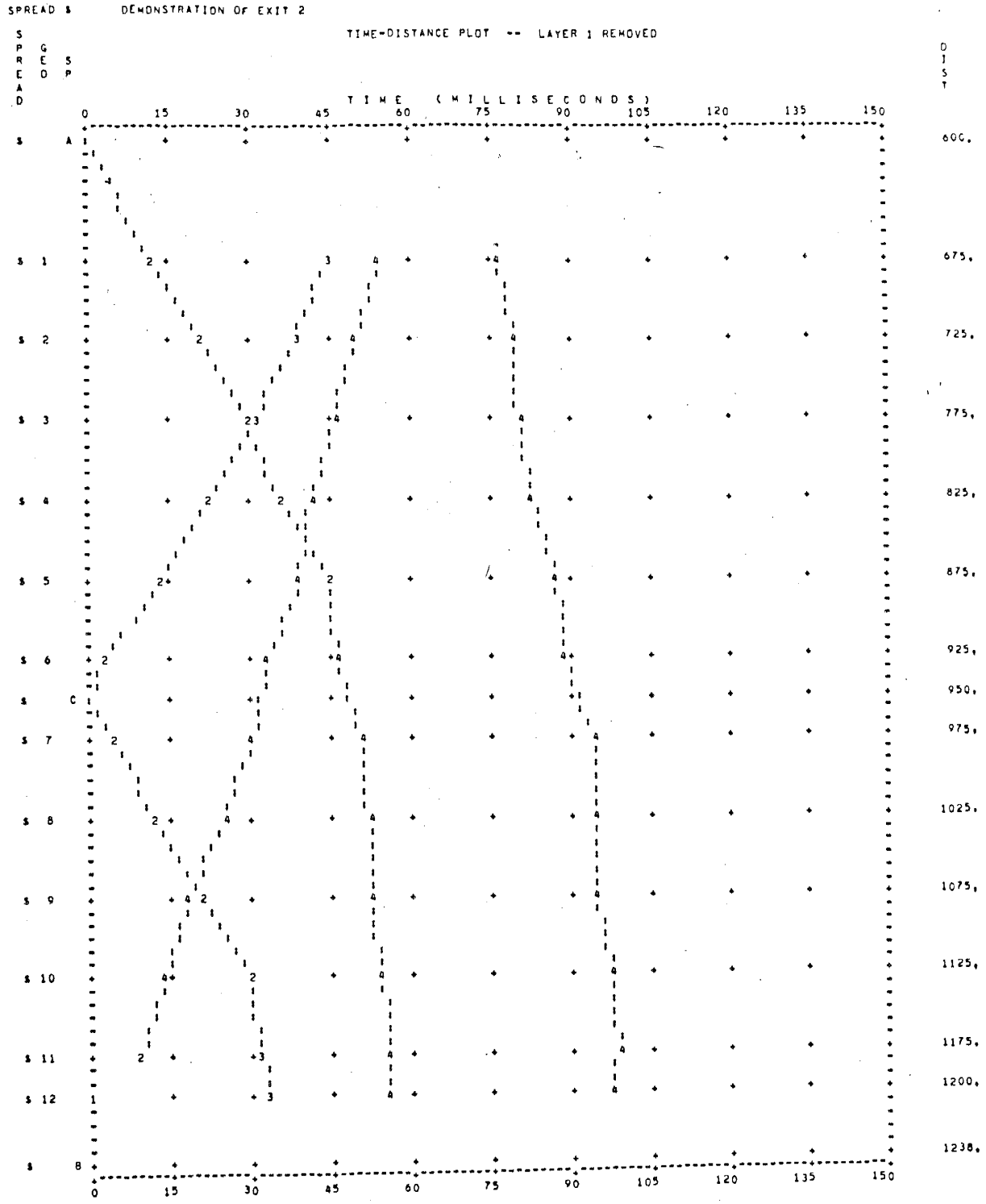

FIGURE 11. Printer Plot, Program FSIP1 EXIT = 2, Showing Time-Distance Graph With the Effects of the Surface Layer Removed.

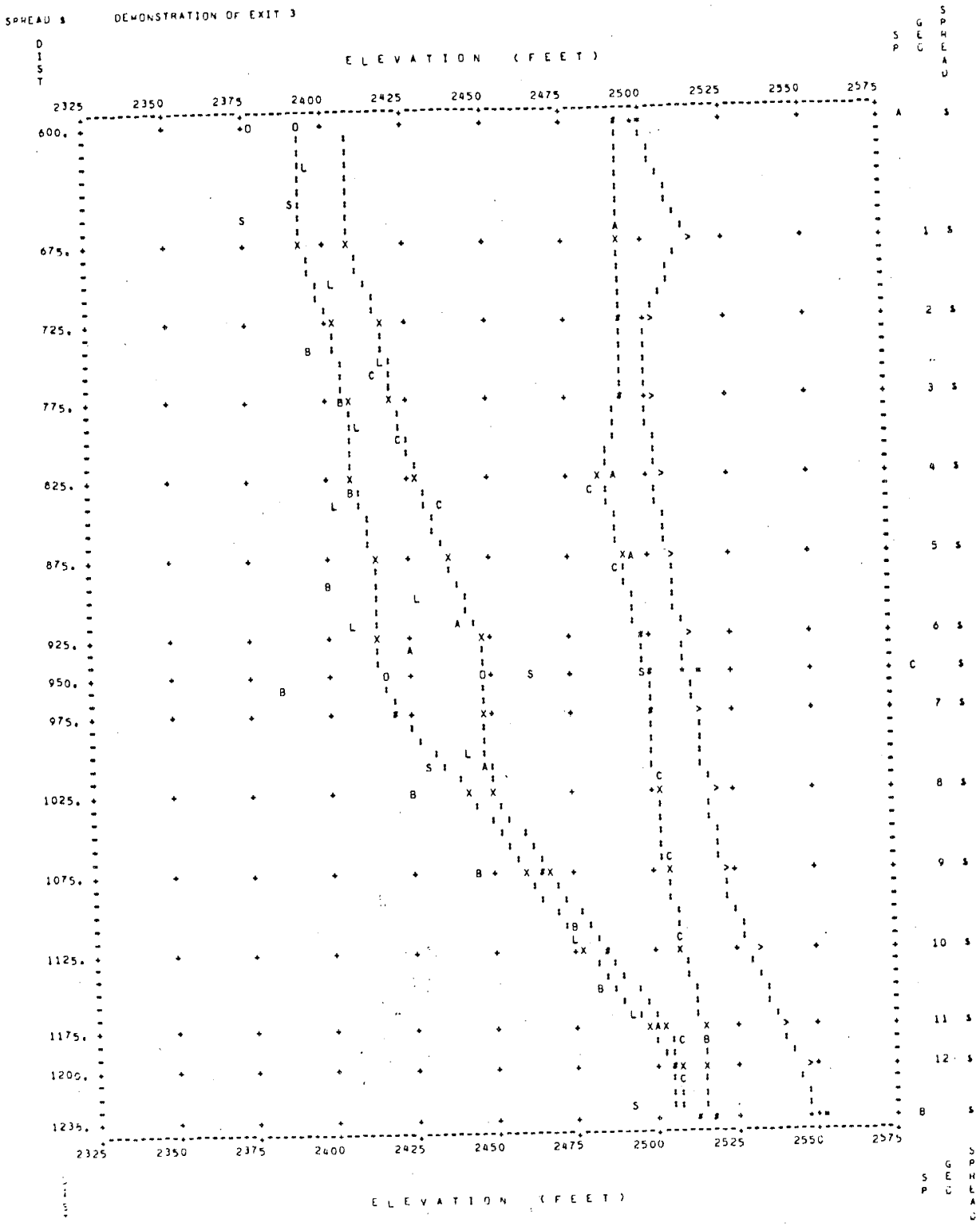

FIGURE 12. Printer Plot, Program FSIP1 EXIT 3, Showing Results of First Approximation Made by Modified Delay Time Computation.

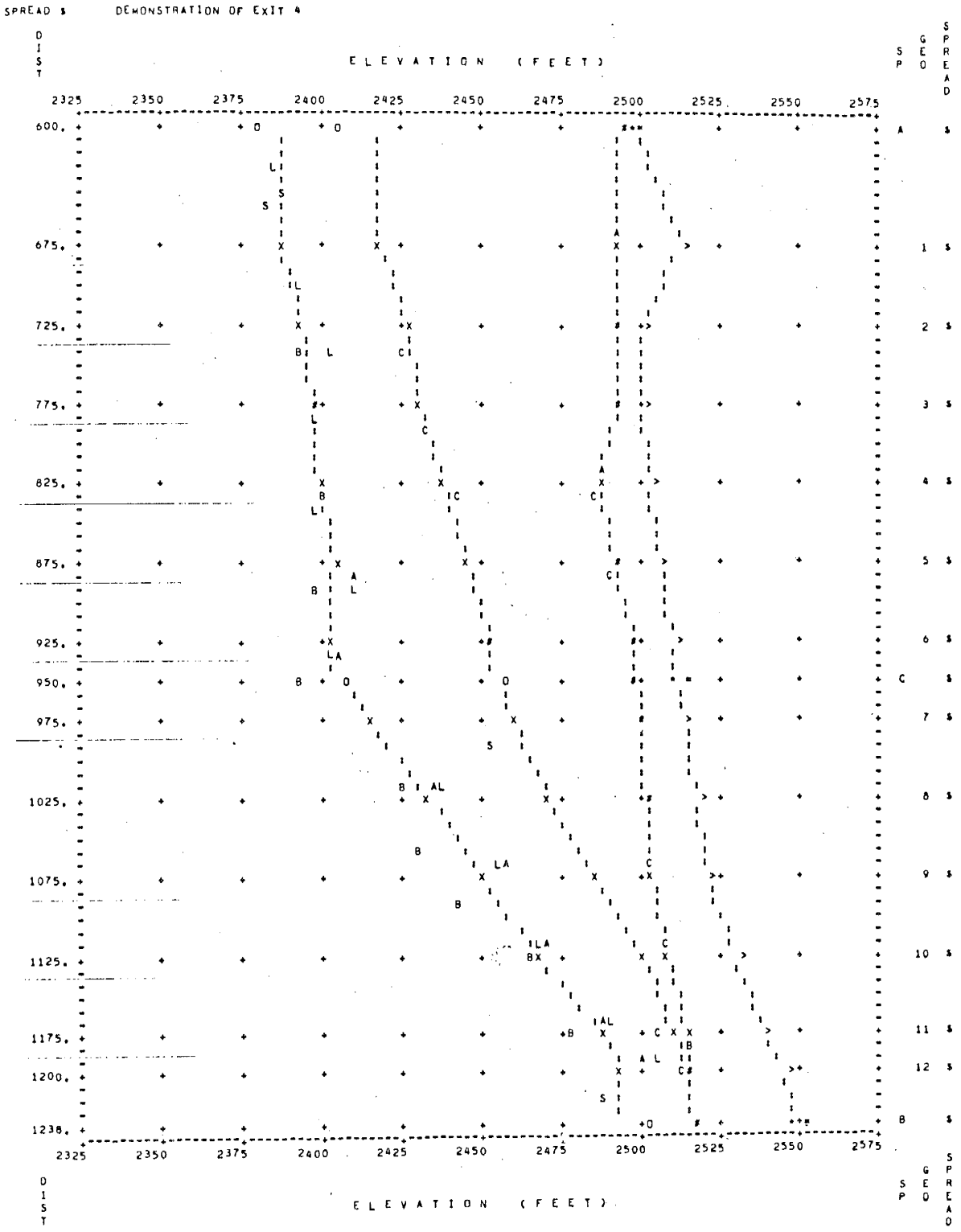

FIGURE 13. Printer Plot, Program FSIP1 EXIT 4, Showing Results of Delay Time Computation Followed by One Pass of Ray-Tracing Adjustment.

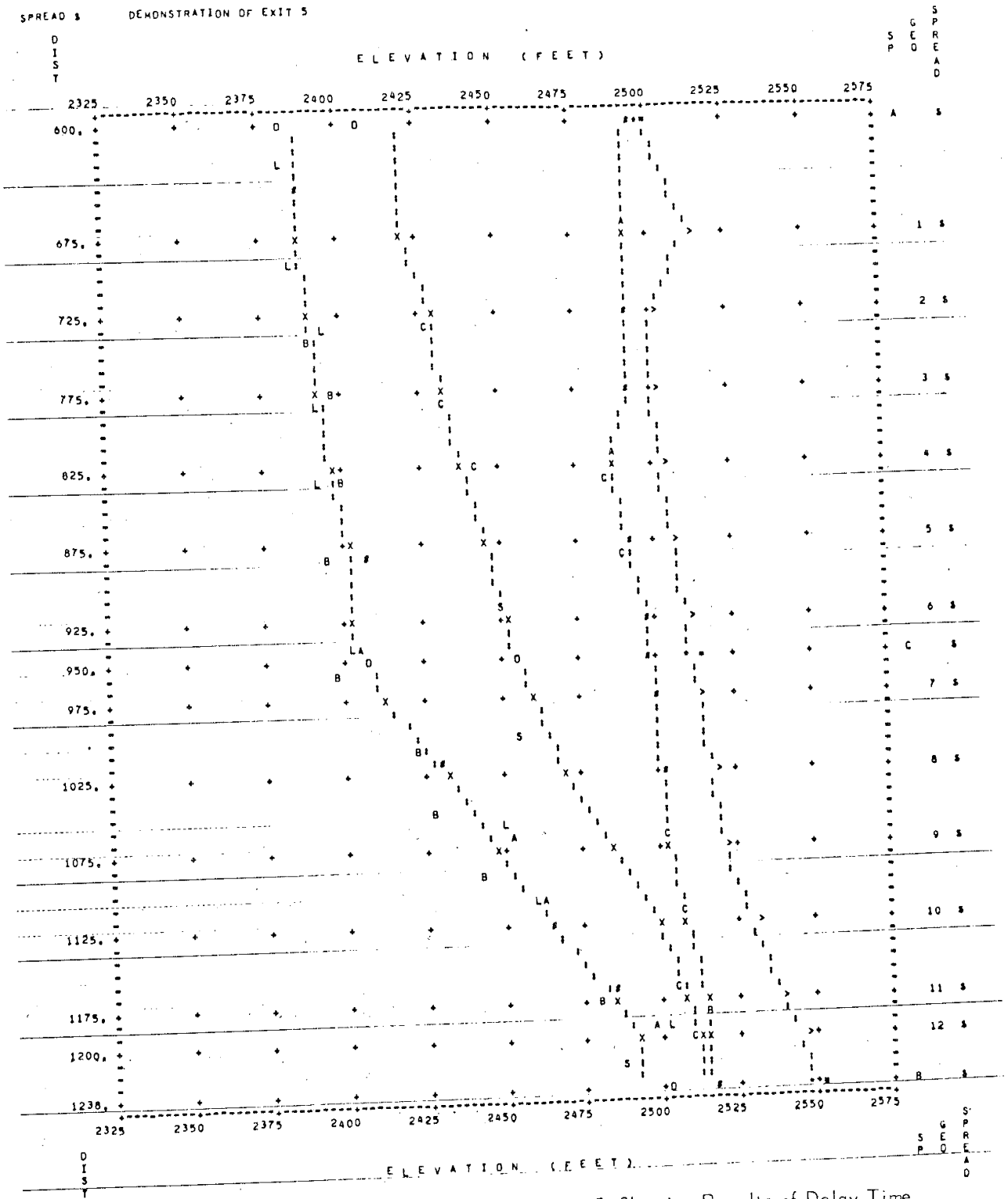

FIGURE 14. Printer Plot, Program FSIP1 EXIT = 5, Showing Results of Delay Time Computation Followed by Two Passes of Ray-Tracing Adjustment.

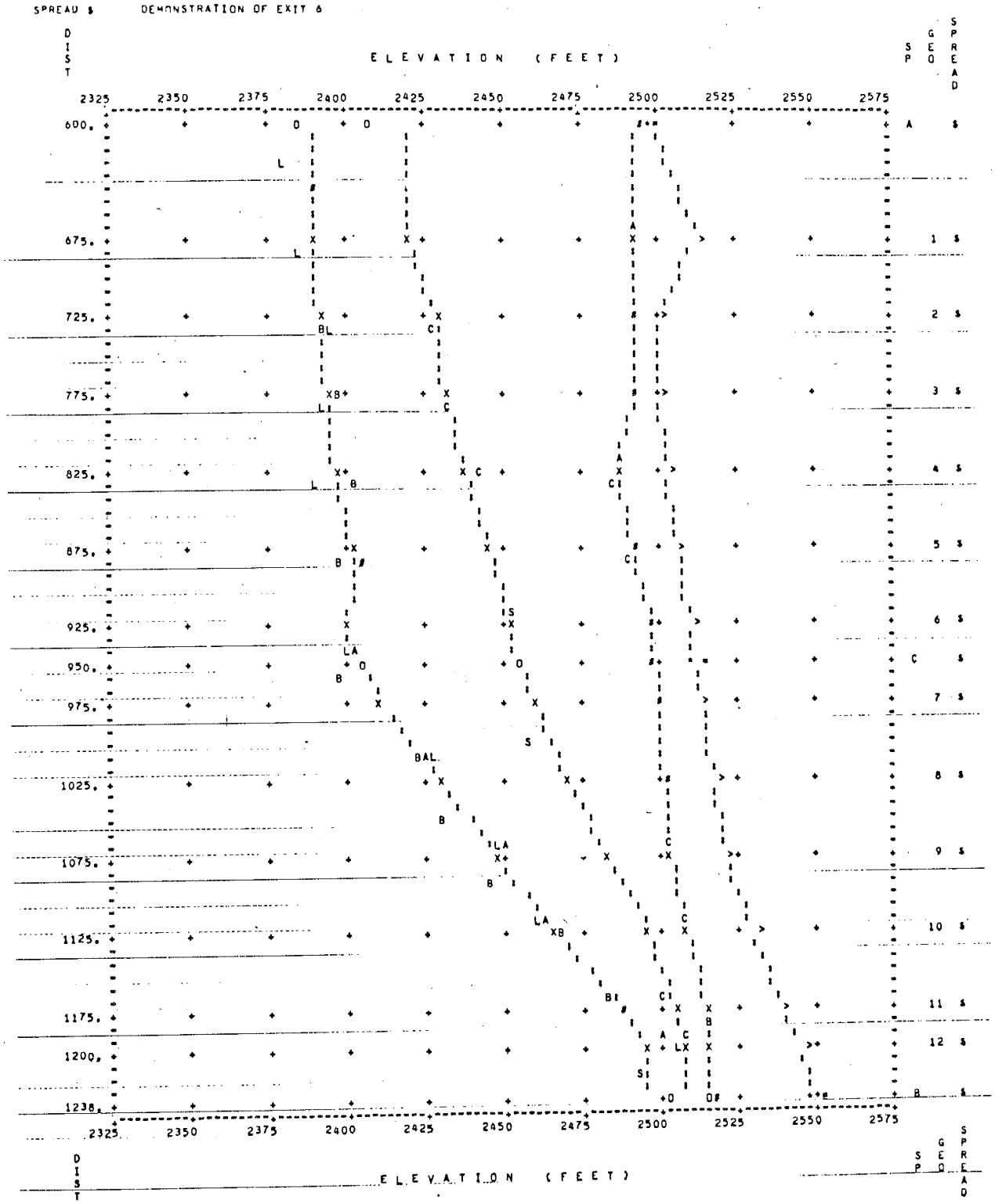

FIGURE 15. Printer Plot, Program FSIP1 EXIT = 6, Showing Results of Delay Time Computation Followed by Three Passes of Ray-Tracing Adjustment.

FIGURE 16. Printer Plot, Program FSIP1 EXIT = 6, Demonstrating Print Option IFILL = 1 Which Causes Layer Number To Fill in Layers.

MODEL STUDIES OF THE REFRACTION PROBLEM

The Fortran Seismic Interpretation Program I is the name of the computer program on which this study was based. The plots shown in the last section are some example data. In order to validate the accuracy of this computer program, six models of different structures were tested. All models were constructed as two-layer systems. The travel times of the compressional waves in each model were determined analytically and plotted on time-distance graphs. Then, travel times were punched on data cards,and these cards were processed by computer program. There are seven optional exits for this computer program. The first EXIT 0 option was selected for checking the time-distance graphs of the models. Then, the EXIT 6 was selected to show the complete data processing. The printer plots were compared to each of the structural models. Each set of data was processed twice. During the first processing, the velocity cards of layers were specified. For the second processing, the layer velocity cards were taken off. If the velocity cards are not included in the problem deck, the computer generates velocity values from the computer program which are used for the interpretation.

General Models

Model 1: Dipping Bed, A one spread model constructed for the dipping bed case is shown in Fig.17. The surface of the refracting bed declines 10 degree to the horizontal. A spread 900 feet long consists of 10 geophones lying in line on the surface. The geohpone interval spacing is 100 feet. The shot points, X and Y are located in line at both ends of the spread at a distance of 100 feet from geophones 1 and 10, respectively. A layer of velocity 5,000 feet/second lines above a layer of velocity 10,000 feet/second. Because of the dipping interface, the down-dip velocity (V_{2d}) is 7,778.6 feet/second and the up-dip velocity (V_{2u}) is 14,619.0 feet/second.

Model 2: Faulted Bed, In this model, a deep high-velocity bed is faulted down. As shown in Fig.18, the fault is assumed to be at the middle point of model. The amount vertical throw is 50 feet. The upper layer of velocity 5,000 feet/second lies above a layer of velocity 10,000 feet/second (see Fig. 18).

Model 3: Folded Bed, As a third model, a structure consisting of a horizontal bed of velocity 5,000 feet/second lying on a folded bed of velocity 10,000 feet/second was considered. As shown in Fig.19, the vertical displacement of the bulge is 100 feet. The spread in model 3 consists of 12 geophones and all geophones are in line. The time-distance

graph shows step down and step up segments as a result of the bulge or fold in layer 2.

Model 4: Dipping and Faulted Bed, The model diagrammed in Fig.20 is a combination of the features of Model 1 and Model 2. The upper layer of velocity 5,000 feet/second lies above the layer of velocity 10,000 feet/second. The higher-velocity layer dips 10 degrees downward and shows a fault at the middle point of the model. The vertical displacement on the fault is 100 feet.

For this model, the down-dip velocity (V_{2d}) is 7,778.6 feet/second and the updip velocity (V_{2u}) is 14,619.0 feet/second. The offset in the time-distance curve (Δt) = 17.1 milliseconds.

Fig. 17 MODEL 1 (DIPPING BED)

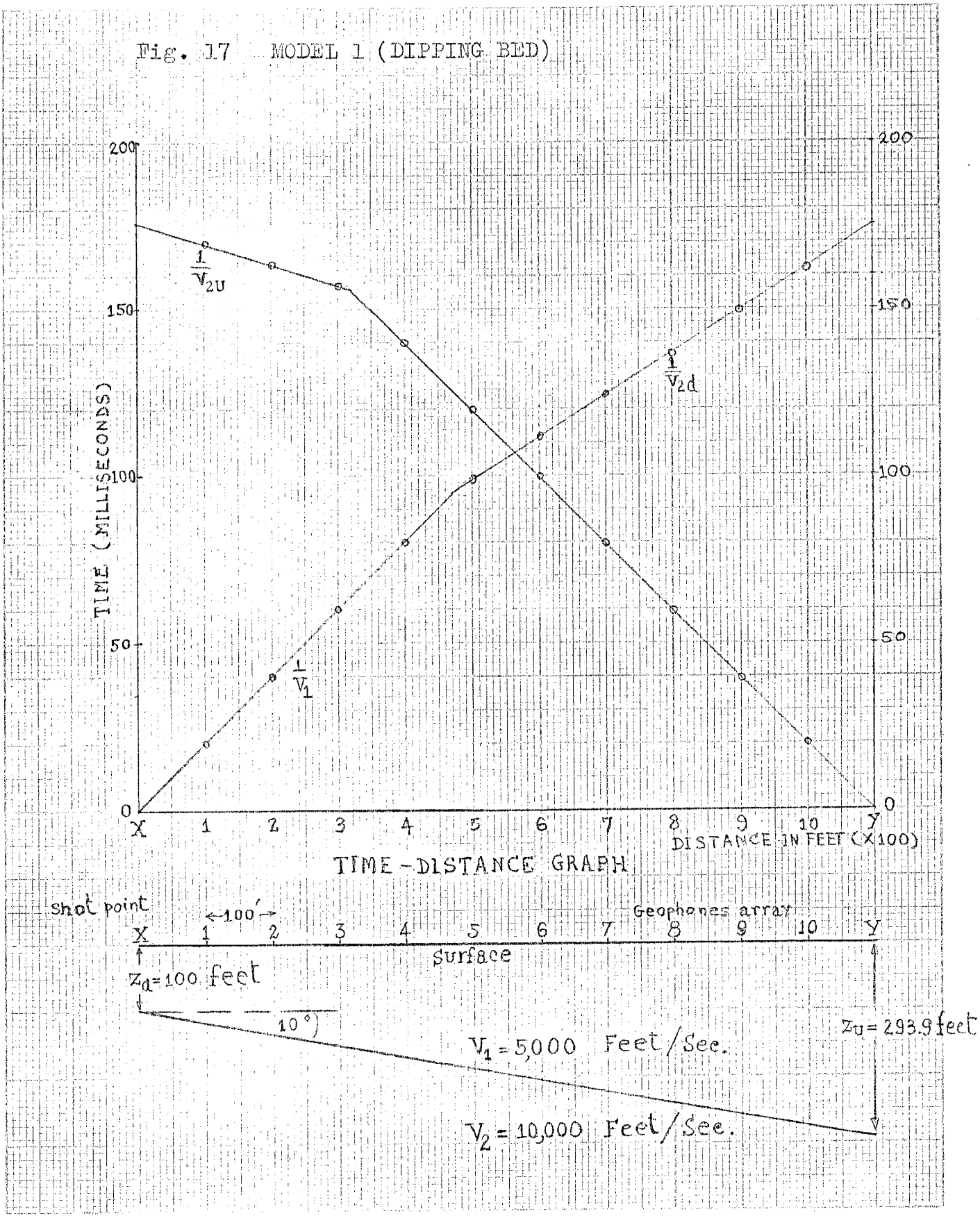

Fig. 18 MODEL 2 (FAULTED BED)

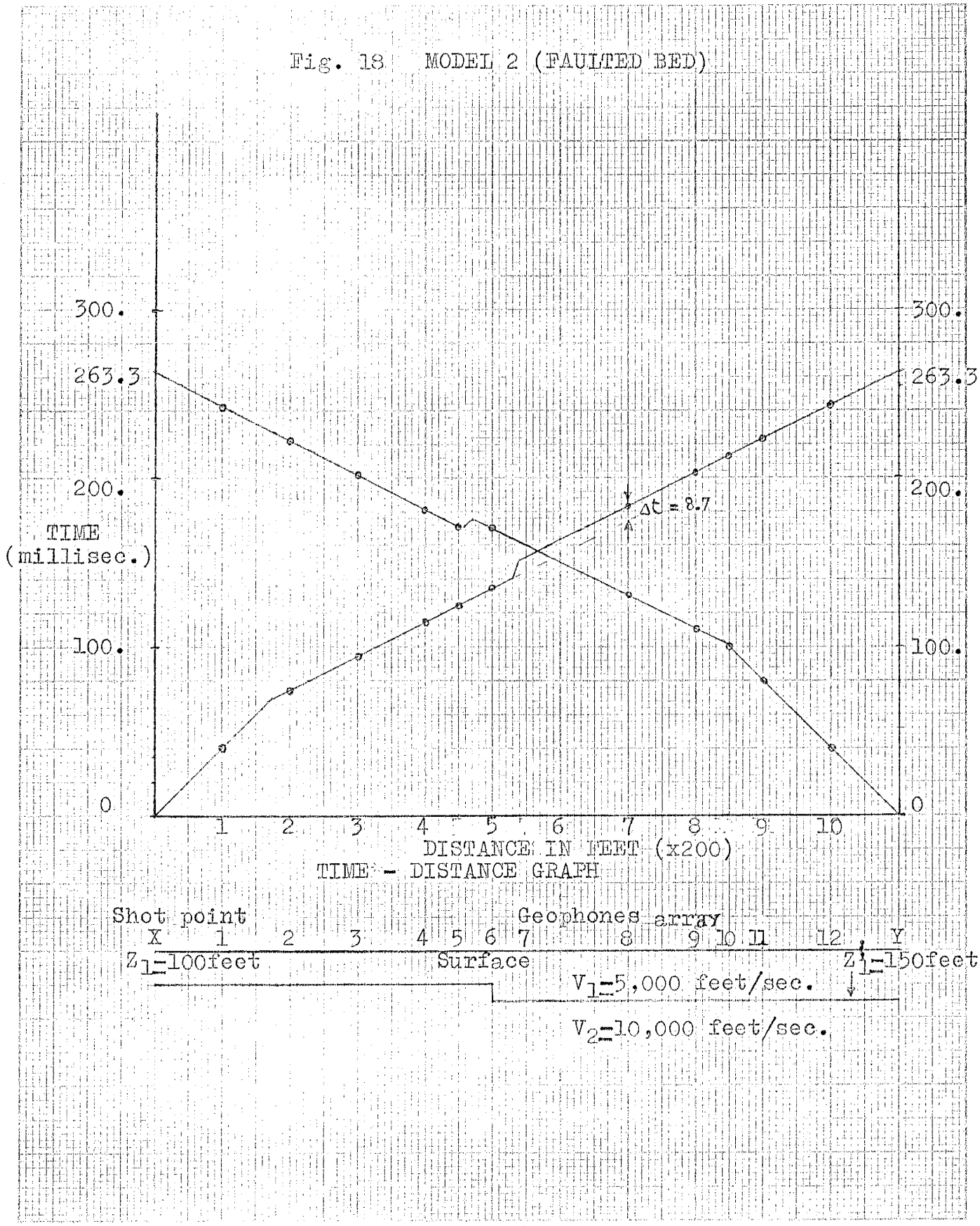

Fig. 19 MODEL 3 (FOLDED BED)

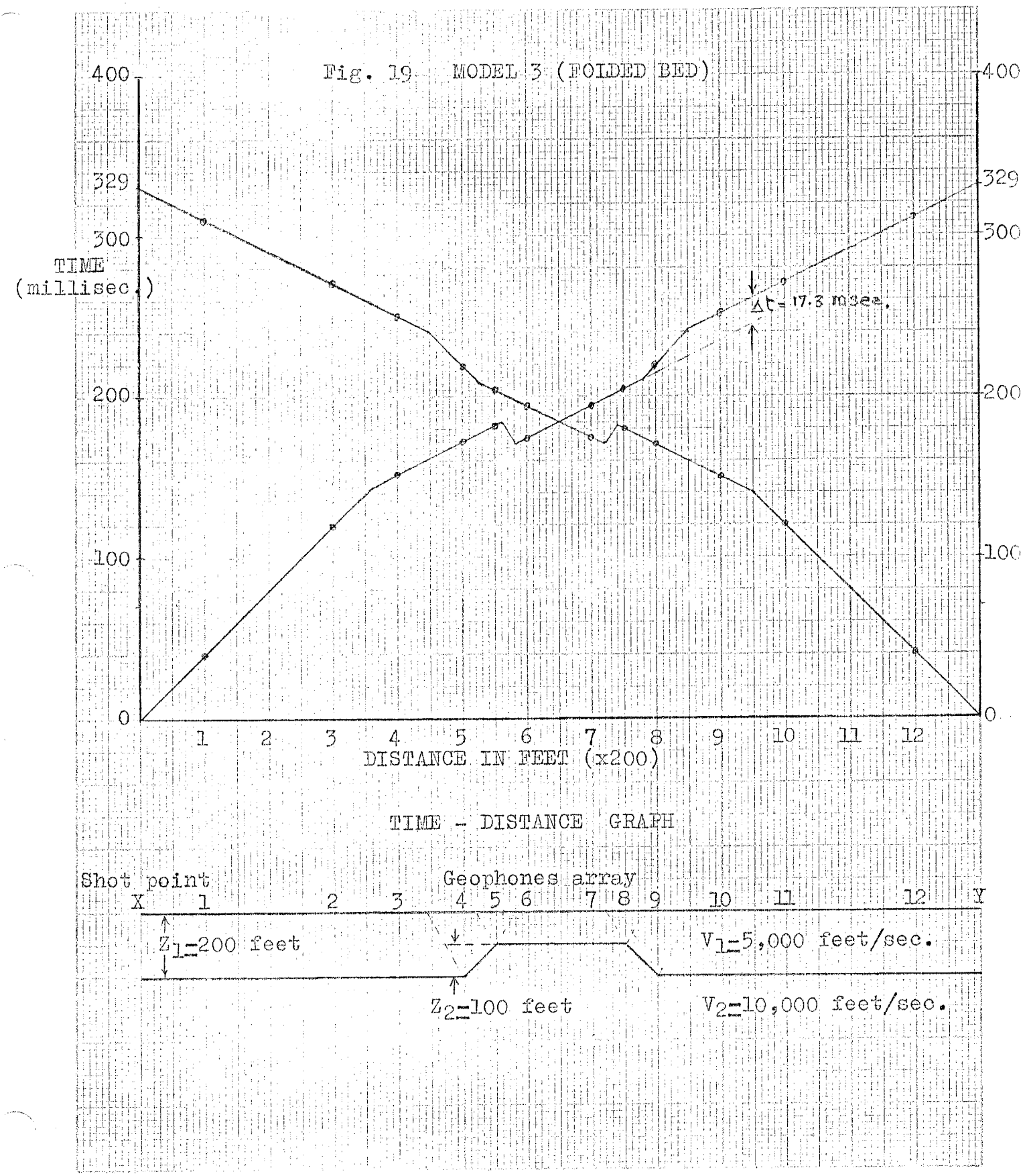

Fig. 20 MODEL 4 (DIPPING AND FAULTED BED)

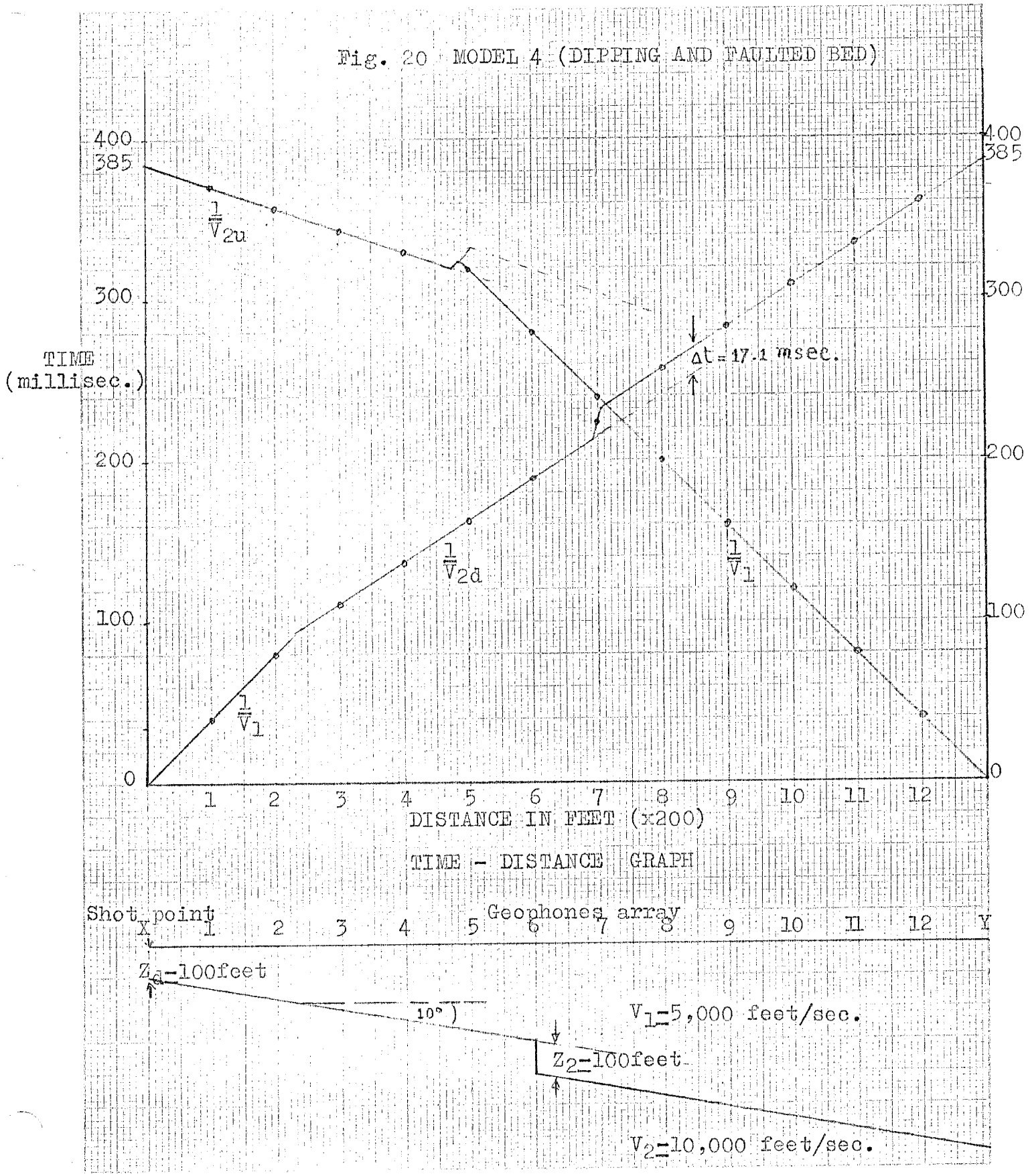

Results Model 1 through 4

The results obtained from the computer program coincide closely with the models for the case of the faulted bed or the folded bed (Models 2 and 3).

For Models 2 and 4, the evidence of a fault does not show sharply because the computer traces the line of the layer by connecting the depth directly to the geophones. When the geophones are arranged along the line with large inter-spacing (greater than 100 feet), and if the fault is located within that distance, the trace of the fault will be smoothed out. In this case, the structural irregularity can be observed from the different depths of the lower layer indicated by two adjacent geophones.

For the case of the dipping bed (Models 1 and 4), the results of the computer interpretation are not accurate, because it indicates a shallower depth than the analytical structural model. The indicated depth is too small by 10 to 30 percent. When layer velocity is specified, the results of the interpretation are more accurate than when no layer velocity is specified.

Note: Model 4 , computer results appear dramatically different than analytical results.

Restriction Models

One restriction of the computer program is that all layer boundaries are assumed to be represented by a series of straight line segments connected end to end beneath the geophone locations and extending from one side of the model to the other. Model 5 and Model 6 are two particular structures of non-homogeneous layers. The compressional wave velocity is changed abruptly in the same layer.

Model 5: Non-Homogeneous Upper Layer, Consider the structural model diagrammed in Fig.21. The compressional wave velocity of an upper layer 30 feet thick is changed abruptly from 1,000 feet/second to 5,000 feet/second. The upper layer overlies a homogeneous layer of velocity 10,000 feet/second. The model is based on one spread of 12 geophones. Two shot points, B and E are located at the each end of spread. The travel times of the compressional waves from shot points to each geophone are plotted in time-distance graph, and were punched on data cards.

Model 6: Non-Homogeneous Lower Layer, This structural model is similar to Model 5 except an upper layer of 10 feet thickness and constant velocity of 2,000 feet/second overlies a non-homogeneous layer. The compressional wave velocity of the lower layer is changed abruptly from 4,000 feet/second to 10,000 feet/second. Geophones and shot points are located as shown in Fig.22.

Fig.21 MODEL 5 (NON-HOMOGENEOUS UPPER LAYER)

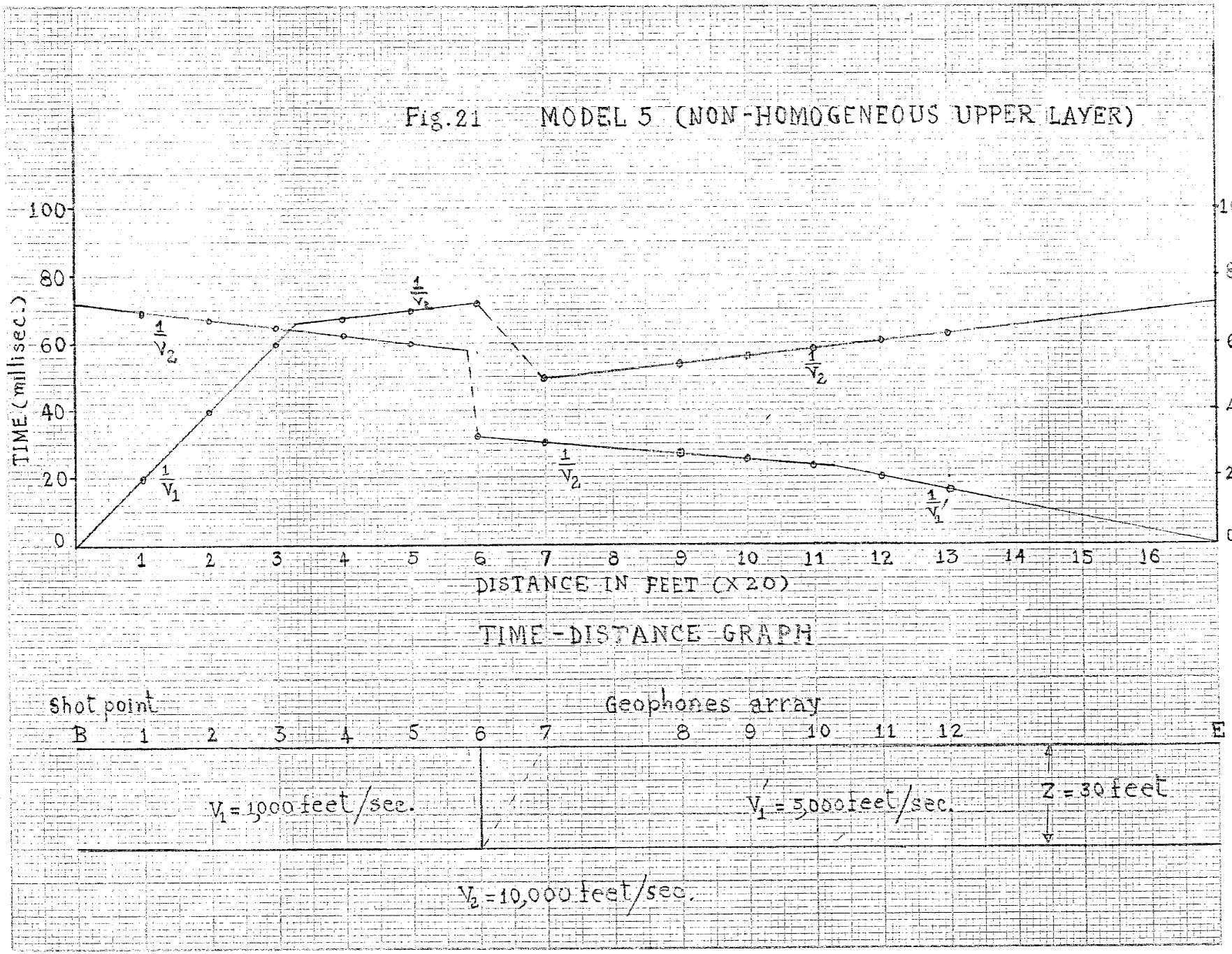

Fig. 22 MODEL 6 (NON-HOMOGENEOUS LOWER LAYER)

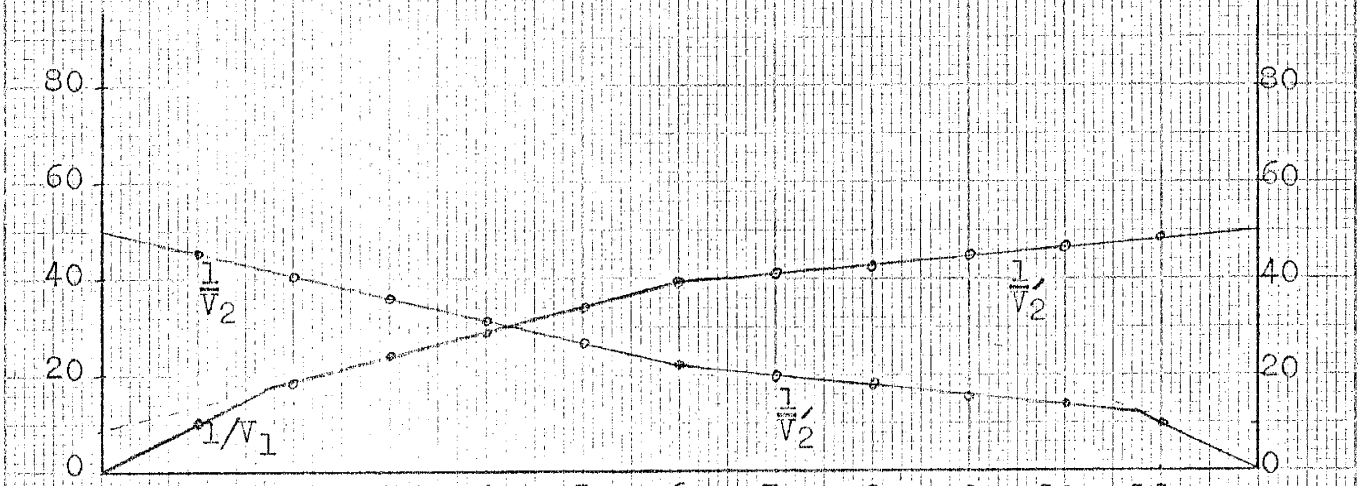

TIME - DISTANCE GRAPH

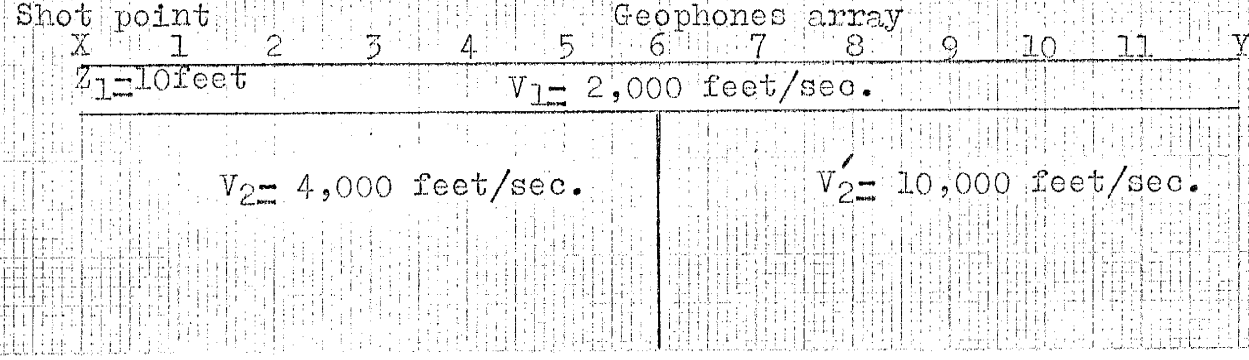

Fig. 23 MODEL 7

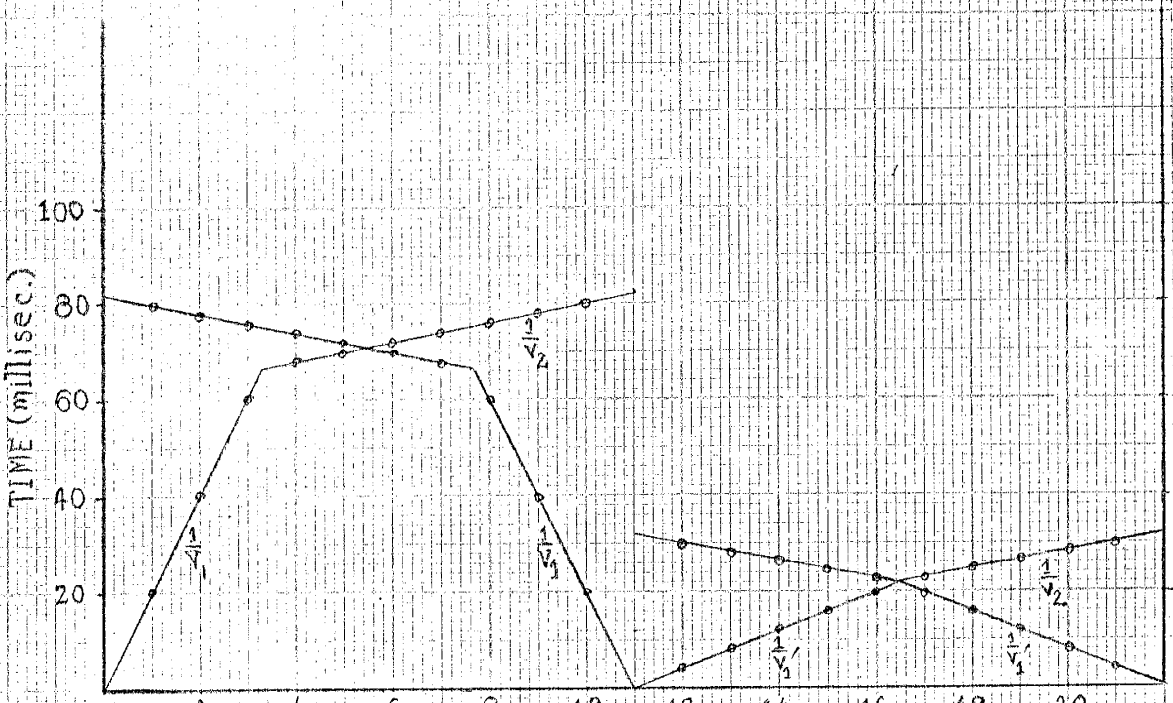

TIME-DISTANCE GRAPH

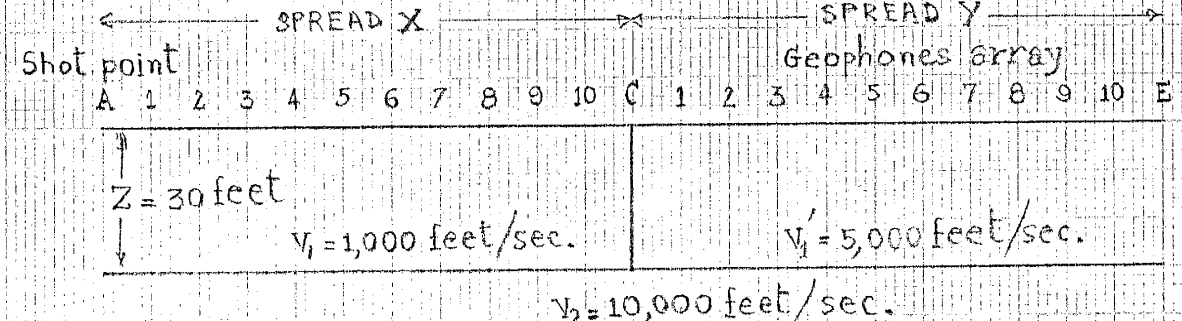

Results Models 5 and 6

The printer plot of the computer interpretation indicates that the computer program does not give satisfactory results for structural irregularities of the type in Models 5 and 6.

The program cannot handle changes of velocities in a layer underlying one spread. The compressional wave velocity of the non-homogeneous layer is treated as an average value. For example in Model 5, the velocity of the upper layer will be (1,000 + 5,000)/2 = 3,000 feet/second, which is not the real velocity. Thus, the result of the interpretation will be incorrect. One way to treat this particular case is to separate the profile into two spreads which are joined end to end at the point of changing velocity. This arrangement is demonstrated in Model 7.

Model 7: Model 7 assumes a structure similar to Model 5. The procedure of interpretation is to separate the model into two spreads, X and Y. Both spreads are joined end-to-end at the point of changing velocity (see Fig.23). Layer velocity cards are specified for both spreads. For spread X Of the upper layer, we specify a velocity of 1,000 feet/second and for spread Y of the upper layer, we specify a velocity of 5,000 feet/second. In the lower layer, both spreads have an equal velocity of 10,000 feet/second.

The printer plot interpretation agrees exactly with the structure of the model (see attached printouts for No.7). Experience has indicated that the computer program can be used to interpret the structure of non-homogeneous systems if the user divides the profile into various spreads for which the layer velocities can be specified.

TWO LAYER SEISMIC PROFILE AT NEW MEXICO INSTITUTE OF MINING & TECHNOLOGY

A refraction profile of 8,200 foot length located at New Mexico tech was used to determine the depth of the water-table. The profile consisted of 103 equally spaced stations of 80 foot separation. Twenty six shots were taken along the profile (Fig.25). The depth profile was computed by hand and reported by Mr. Abou Bakr K. Ibrahim in his thesis for a Master of Science degree at New Mexico Institute of Mining and Technology.

The computer program was applied to the seismic refraction data obtained by Ibrahim. The printer plot of the depth profile obtained from the computer program was compared to the depth profile given by Ibrahim.

Ibrahim's Interpretation

By following standard methods of interpretation seismic refraction (Dix, 1952), Ibrahim obtained the depth profile shown in Fig.26. The topography of the profile is inclined slightly from an elevation of 4,850 feet to 4,650 feet from station 1 to station 104. The thickness of the upper layer is about 110 feet at station 1 and the depth gets gradually shallower along the profile until it is about 60 feet deep at the station 104, except the part between the station 13 to station 43 which shows a structural uplift of about 50

feet between vertical faults. The measured seismically determined depths at some positions along the profile agree closely with depths measured to water at two wells located a few hundred feet from the profile.

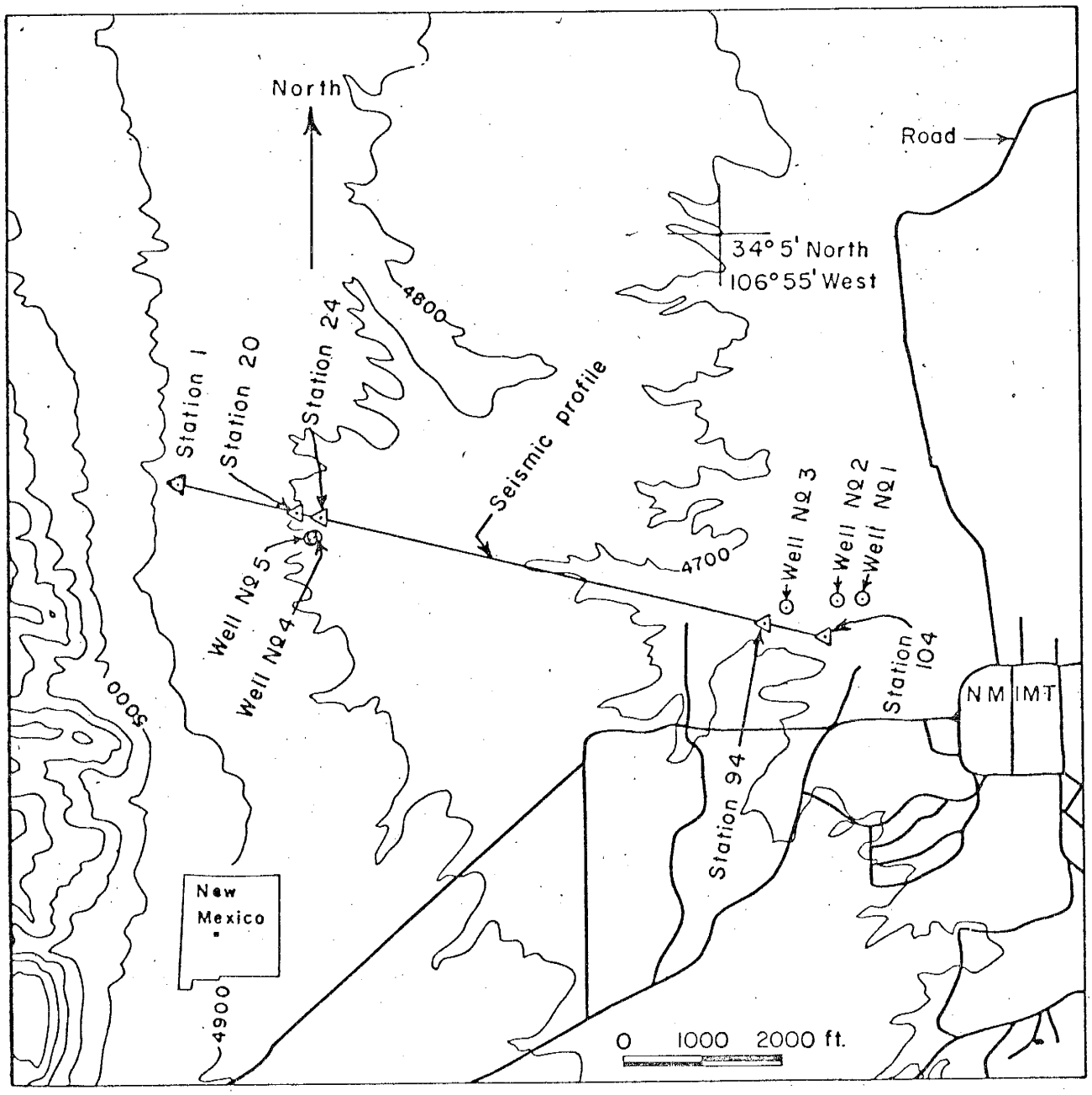

Fig.24 Index map showing location of the area, seismic profile, and wells used in the tests.

Fig.25 Time-distance curves.

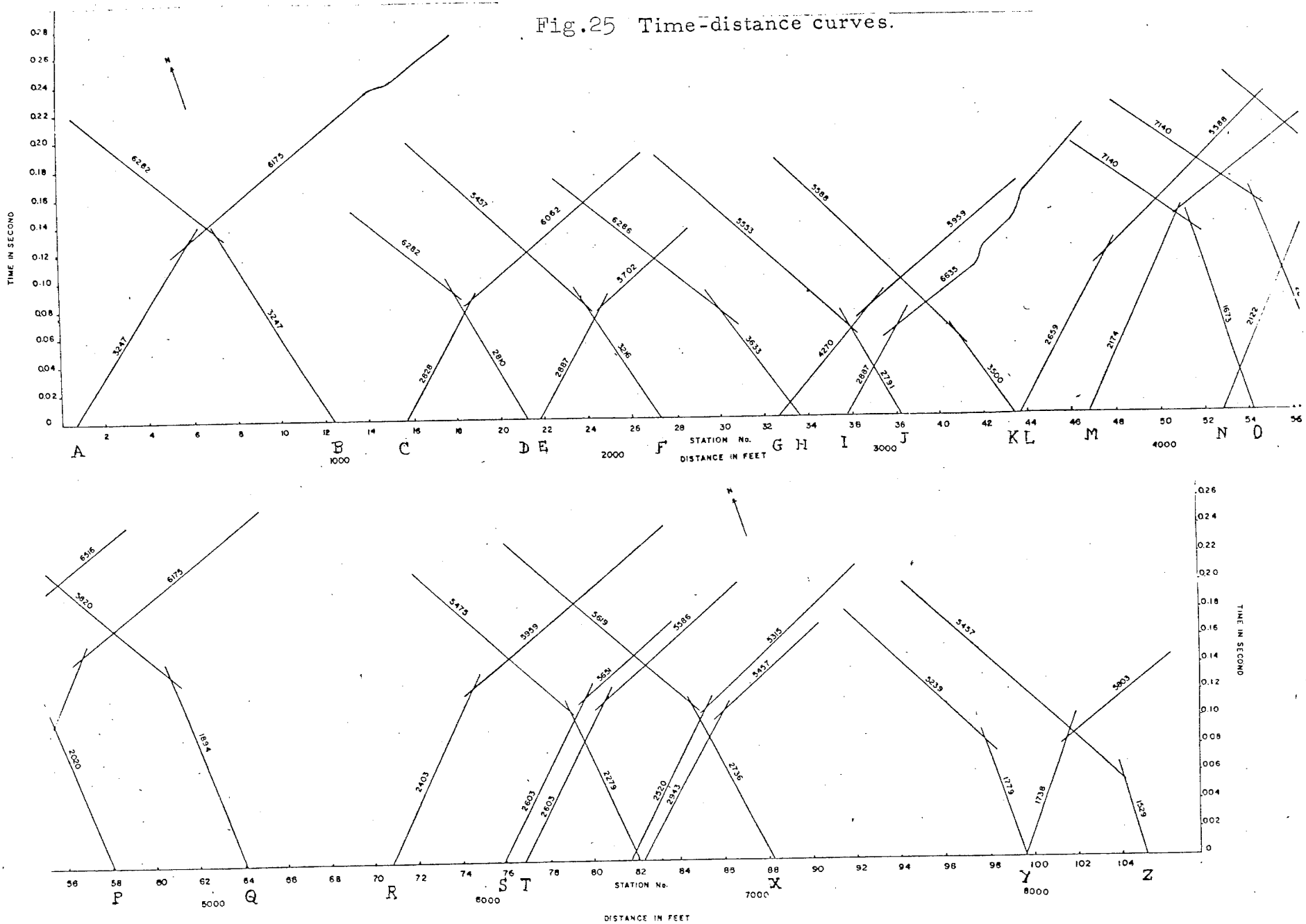

Fig.26 Hand calculated depth profile and locations of wells No. 3 and No. 5.

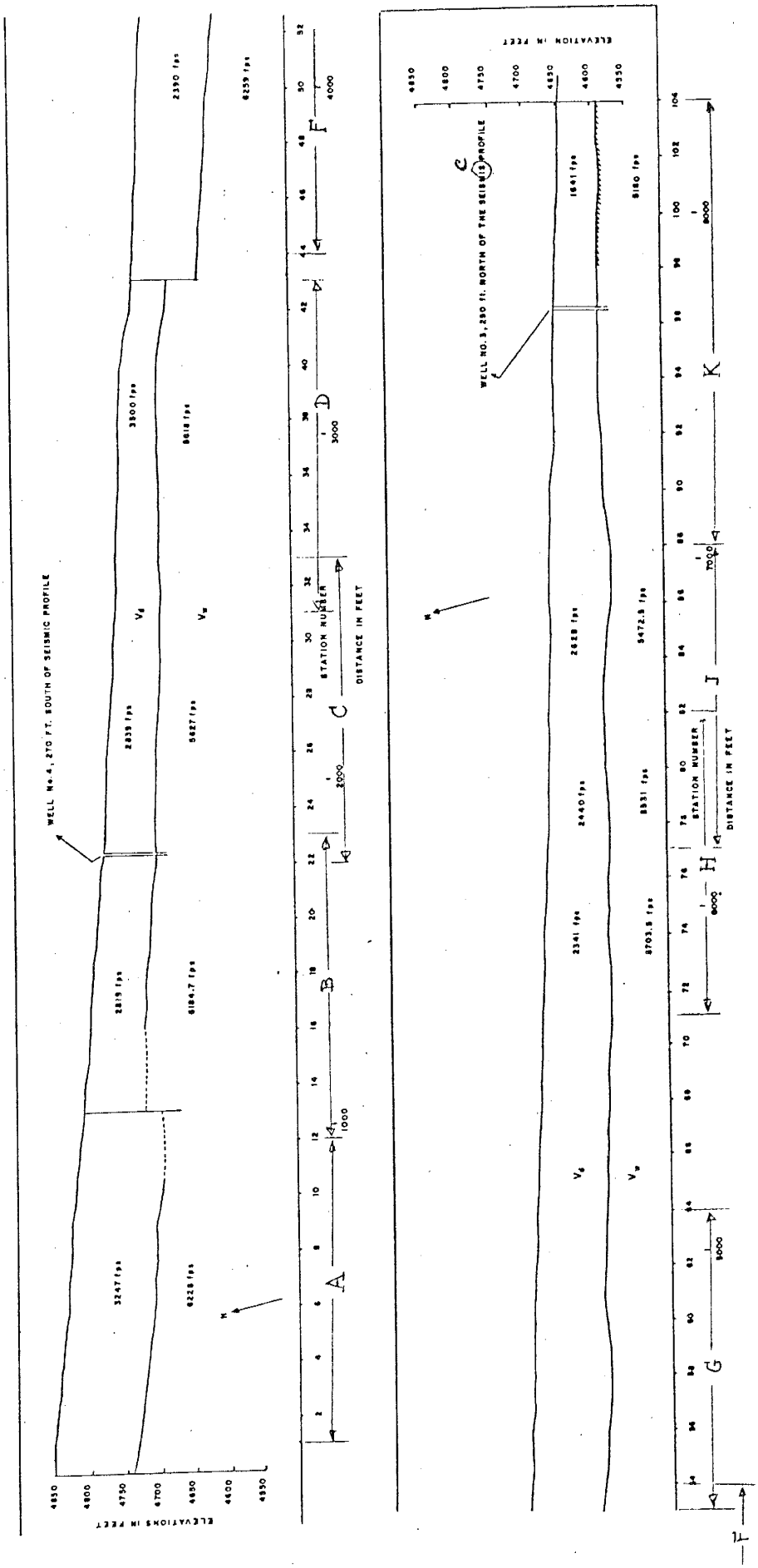

Computer Program Interpretation

Data for the computer program was obtained from the time-distance graph in A.R. Sanford's offic. Because the profile was very long, the interpretation was separated into three problem decks. After the processing, all of printer plots of the depth cross-section profiles were joined together. Each problem deck data consisted of 3 spreads. Missing travel times were found by interpolation and extrapolation of data on the time-distance curve.

I) The first problem profile of 2,560 feet long consists of three spreads called A, B, and C. The distance between each geophone in each spread was 80 feet. The printer plot of the cross-section (see attached printouts for No.8) fairly well matched the results obtained by Ibrahim. Along this profile, a difference in the results was noticed at only one location, at the 960 foot mark on the profile. On the original time-distance graph, there is no clear evidence of a fault. The trace of the refracted layer is almost a straight line on the time-distance graph. Therefore, no faulted bed is shown in the computer profile.

II) The second problem profile of length 2,650 feet consists of three spreads called D, F,and G. All spreads are in line with one another, spread D and spread F are separated by 80 feet but spread F and spread G are overlaped 80 feet. Geophones are spread along the profile at 80 foot spacing

intervals.

The printer plot of the depth cross-section profile,(see attached printouts for No.9) similarly, is close to the depth profile obtained by hand calculations. The results differ at only two points. The computer generated plots show evidence of two faults at the distances 880 feet, and 1,200 feet from the beginning of the profile, but the hand calculated profile shows only one big step fault at the distance 960 feet. The depths of the surface layer obtained by the two methods, are very close but the computer depths are deeper at the beginning of the profile than the hand calculated depths.

III) The third problem profile of length 2,650 feet is separated from the second profile by about 560 feet. The data are for three spreads called H, J, and K. Spread H is overlaped 400 feet with spread J but spreads J and K are joined end-to-end. The profile generated by the printer (see attached printouts for No.10) shows results amazingly close to the hand calculated profile.

CONCLUSIONS

Depth computations from the computer program give accurate results for the case of structures consisting of horizontal bedding. In the case of faulted horizontal bed, the computer plots are fairly accurate. The computer traces the line of the lower layers by connecting the depth directly beneath every geophone, and tends to smooth out sharp drops in the structure. Thus, the evidence of a fault is not shown clearly. However, from the difference between elevations of nearby positions, the location of a fault can be found.

For the case of a dipping bed, the velocities of the compressional wave along the updip shooting are greater than from along downdip shooting and both are apparent velocities. The depth computation for this case is a more complex procedure, which the computer program cannot handle correctly. The error in the computer for dipping beds results may be 10 to 30 percent.

In general, layers in the earth's crust are not homogeneous. Various valus of compressional wave velocities may be detected in the same layer. Computer results for this case are very poor unless the time-distance data is rearranged. The latter procedure requires prior knowledge of what the structure is.

REFERENCES

1. Scott, J. H., Tibbetts, B. L., Burdick, R. G. (1972) Computer Analysis of Seismic Refraction Data, Report of Investigation 7595, Bureau of Mines, United States Department of The Interior, 95 p.

2. Sanford, Allan R. (1972) Geophysics 445, Notes for Study in Glass, pp. 23-34.

3. Nettleton, L. L. (1940) Geophysical Prospecting for Oil, McGraw-Hill Book Co., New York, 444 p.

4. Dobrin, M. B. (1960) Introduction to Geophysical Prospecting, McGraw-Hill Book Co., New York, 446 p.

5. Dix, C. H. (1952) Seismic Prospecting for Oil, Harper and Brothers, New York, 414 p.

6. Bacon, Lloyal O. (1966) Refraction Seismic Case Histories in Mining Geophysics, In Mining Geophysics, v.1, Case Histories, Society of Exploration Geophysics, Tulsa, Okla., pp. 105-113.

7. Ibrahim, Abou-Bakr K. (1962) Relation Between Compressional Wave velocity and Aquifer Porosity, Thesis of Master of Science, New Mexico Institute of Mining and Technology, pp. 1-8.